ISTANBUL TECHNICAL UNIVERSITY ★ GRADUATE SCHOOL

COMPARATIVE ANALYSIS OF PHYSICS-BASED MODELS FOR LITHIUM-ION BATTERIES IN E-MOBILITY APPLICATIONS

M.Sc. THESIS

Hakkı YAVUZ

Department of Electrical Engineering

Electrical Engineering Programme

JULY 2024

ISTANBUL TECHNICAL UNIVERSITY ★ GRADUATE SCHOOL

COMPARATIVE ANALYSIS OF PHYSICS-BASED MODELS FOR LITHIUM-ION BATTERIES IN E-MOBILITY APPLICATIONS

M.Sc. THESIS

Hakkı YAVUZ
(504211021)

Department of Electrical Engineering

Electrical Engineering Programme

Thesis Advisor: Assoc. Prof. Mehmet Onur Gülbahçe

JULY 2024

İSTANBUL TEKNİK ÜNİVERSİTESİ ★ LİSANSÜSTÜ EĞİTİM ENSTİTÜSÜ

E-MOBİLİTE UYGULAMALARI İÇİN LİTYUM-İYON BATARYALARIN FİZİK TABANLI MODELLERİNİN KARŞILAŞTIRMALI ANALİZİ

YÜKSEK LİSANS TEZİ

Hakkı YAVUZ
(504211021)

Elektrik Mühendisliği Anabilim Dalı

Elektrik Mühendisliği Programı

Tez Danışmanı: Doç. Dr. Mehmet Onur Gülbahçe

TEMMUZ 2024

Hakkı YAVUZ, a M.Sc. student of ITU Graduate School student ID 504211021 successfully defended the thesis entitled "COMPARATIVE ANALYSIS OF PHYSICS-BASED MODELS FOR LITHIUM-ION BATTERIES IN E-MOBILITY APPLICATIONS", which he/she prepared after fulfilling the requirements specified in the associated legislations, before the jury whose signatures are below.

Thesis Advisor :	**Assoc. Prof. Mehmet Onur Gülbahçe** Istanbul Technical University	....
Jury Members :	**Asst. Prof. Cavit Fatih Küçüktezcan** Istanbul Technical University	....
	Asst. Prof. Mustafa Alparslan Zehir Marmara University	....

Date of Submission : **22 May 2024**
Date of Defense : **5 July 2024**

To my family and loved ones,

FOREWORD

I really want to thank my family and friends for their never-ending and relentless support. I would also like to thank my thesis advisor Assoc. Prof. Mehmet Onur Gülbahçe for his support, patience and guidance.

For the most special, my girlfriend Müzeyyen Nur Kaplan's support, belief and love have always been the greatest motivation for me.

July 2024 Hakkı YAVUZ

TABLE OF CONTENTS

ABBREVIATIONS

BEV	: Battery Electric Vehicle
BMS	: Battery Management System
ECM	: Equivalent Circuit Model
EVs	: Electric Vehicles
HEVs	: Hybrid Electric Vehicles
HW-FET	: Highway Fuel Efficiency Test
IEA	: International Energy Agency
LiBs	: Lithium-ion Batteries
LiCoO2	: Lithium Cobalt Oxide
LiFePO4	: Lithium Iron Phosphate
Lipo	: Lithium Polymer
NMC	: Lithium Nickel Manganese Cobalt Oxide
NYCC	: New York City Cycle
NREL	: National Renewable Energy Laboratory
OCV	: Open Circuit Voltage
ODEs	: Ordinary Differential Equations
PDEs	: Partial Differential Equations
PHEVs	: Plug-in Hybrid Electric Vehicles
SOC	: State of Charge
SOH	: State of Health

SYMBOLS

α	:	Alpha
β	:	Beta
R	:	Resistance (Ohm)
C	:	Capacitance (Farad)
L	:	Inductance (Henry)
V	:	Voltage (Volt)
I	:	Current (Ampere)
P	:	Power (Watt)
Z	:	Impedance (Ohm)
f	:	Frequency (Hertz)
V_{oc}	:	Open Circuit Voltage
I_{sc}	:	Short Circuit Current
V_{term}	:	Terminal Voltage
P_{max}	:	Maximum Power
C_{rate}	:	C-rate (Charge/Discharge Rate)
E_{bat}	:	Battery Energy
P_{bat}	:	Battery Power
SOC	:	State of Charge
DOD	:	Depth of Discharge
R_{int}	:	Internal Resistance

LIST OF TABLES

LIST OF FIGURES

Page

COMPARATIVE ANALYSIS OF PHYSICS-BASED MODELS FOR LITHIUM-ION BATTERIES IN E-MOBILITY APPLICATIONS

SUMMARY

The widespread adoption of electric vehicles (EV) has led to the development of lithium-ion batteries as a critical technological solution due to their high energy density and fast charging capacity. Continued improvement of these batteries will play a key role in achieving the goals of extending EV range, reducing charging times and improving overall performance. However, this technological development is hindered by several challenges.

Battery models are generally classified into four main groups. Empirical models, such as Shepherd, Unnewehr universal, and Nernst, are based on experimental data and offer varying degrees of accuracy and computational complexity. Equivalent Circuit Models (ECM), simplify the representation of the internal electrical characteristics of a battery using circuit elements. They offer flexibility in designing structures suitable for specific applications, but may require more cell information and increase computer time. The data-driven battery modeling based solution utilizes machine learning methods to derive knowledge from large datasets of battery measurements. It excels at modeling complex nonlinear behaviors and provides high accuracy, but requires careful experimental setup and high-quality data. Physics-based models including the Single Particle Model (SPM), the Single Particle Model with Electrolyte (SPMe), and the Doyle-Fuller-Newman (DFN) model describe mathematically the basic physical and chemical phenomena in a battery. In-depth information about battery behavior can be provided and can be used to optimize battery performance. Beside this, as a key part of physics-based models, degradation models are vital in extending battery life and efficiency.

This thesis addresses the physics-based simulation methods of lithium-ion batteries for electric cars, focusing in particular on SPM, SPMe and DFN models. Their performance has been extensively studied and compared with different chemical batteries. Their complexity and predictive capabilities are summarized and evaluated based on literature studies.

The thesis begins with a comprehensive overview of all battery modeling methods. Next, physics based modeling methods for batteries with different chemical compositions are simulated and analyzed in detail. Optimizations are performed to obtain more efficient parameter values due to uncertainty in literature values. All the mathematical formulations needed to build an electric vehicle model are processed and the electric vehicle model is developed using simulation environments. The electric vehicle model is integrated with physics-based modeling methods for battery sizing and range calculation studies. A detailed simulation study is performed using vehicle

models and battery modeling methods. The accuracy and precision of the simulation has been proved by comparing the obtained simulation results with the regional data presented earlier in the literature.The mechanisms that can influence cellular aging are widely studied and these changes are observed in cycles.

Finally, this thesis presents a comprehensive analysis of battery modeling methods for electric vehicles. By comparing the performance of different chemical battery modeling methods and optimizing existing modeling techniques, it contributes to a more accurate and reliable prediction of electric vehicle battery performance. This in turn is a significant step towards extending battery life and increasing the durability of electric vehicles.

The importance and contribution of the thesis is to provide an updated and comprehensive source of information on battery modeling methods. This is one of the few comprehensive studies that compares the performance of battery modeling methods with different chemical batteries. This helped identify the most appropriate modeling methods for batteries with different chemical compositions. It also facilitated more accurate prediction of battery performance by optimizing existing battery modeling techniques. The thesis provided new ideas and basic tools for the design and optimization of electric vehicles and promoted a more sustainable future with information related to extending the battery life of electric vehicles.

E-MOBİLİTE UYGULAMALARI İÇİN LİTYUM-İYON BATARYALARIN FİZİK TABANLI MODELLERİNİN KARŞILAŞTIRMALI ANALİZİ

ÖZET

Elektrikli araçların yaygınlaşmasıyla birlikte, yüksek enerji yoğunluğu ve hızlı şarj özellikleriyle lityum-iyon piller otomotiv endüstrisinde önemli bir teknoloji çözümü haline gelmiştir. Bu pillerin sürekli gelişimi, elektrikli araçların menzilini artırma, şarj sürelerini kısaltma ve genel performanslarını iyileştirme hedeflerinde kritik bir rol oynamaktadır. Ancak, bu teknolojik gelişmelerin önünde çeşitli engeller bulunmaktadır. Özellikle, lityum-iyon pillerin güvenlik endişeleri, maliyet faktörleri, enerji yoğunluğu sınırlamaları ve çevresel etkileri gibi zorluklar hala çözülmesi gereken alanlardır. Ayrıca, pil ömrünün uzatılması ve şarj sürelerinin daha da kısaltılması gibi hedeflere ulaşmak için sürekli yenilik ve araştırmaya ihtiyaç vardır. Bu bağlamda, ileri teknolojilerin geliştirilmesi ve uygulanmasıyla, elektrikli araçların ve lityum-iyon pillerin geleceği daha da parlak hale gelebilir. Ancak, bu süreçte sadece teknik açıdan değil, aynı zamanda ekonomik ve çevresel açıdan sürdürülebilir çözümler de önem taşımaktadır. Bu nedenle, endüstriyel ve akademik paydaşlar arasında iş birliği ve bilgi paylaşımı, elektrikli araç teknolojisinin ve lityum-iyon pillerin evriminde kritik bir rol oynamaktadır. Bu bağlamda, güvenlik, performans, maliyet etkinliği ve çevresel sürdürülebilirlik gibi faktörlerin dikkate alınması, elektrikli araç endüstrisinin geleceğini belirleyecek önemli unsurlardır.

Batarya modelleri literatürde genellikle dört ana kategoriye ayrılır. İlk olarak, deneylere dayanan klasik ampirik modeller, Shepherd, Unnewehr evrensel ve Nernst gibi modelleri içerir. Shepherd modeli, sürekli deşarj akımları için etkili bir şekilde kullanılırken, Unnewehr evrensel modeli genellikle genel bir uygulamaya sahiptir. Öte yandan, Nernst modeli, özellikle doğruluk seviyesiyle öne çıkar ve dinamik terminal voltajı tahmin etmede başarılıdır. Bu modeller arasındaki seçim, özellikle uygulama gereksinimlerine ve hesaplama karmaşıklığına bağlıdır.

İkinci olarak, Eşdeğer Devre Modelleri (ECM), bataryaların içsel elektriksel özelliklerini doğru bir şekilde ayırt etme yeteneklerinde yüksek derecede basitleştirme sergilerler. Ayrıca, birçok devre bileşeni ve bunların varyasyonlarından dolayı, ECM, araştırmacılara uygulamaları için uygun bir yapı tasarlama esnekliği sunar. Ancak, eşdeğer devre içinde daha fazla eleman kullanmanın dezavantajı, hücreye ilişkin daha fazla bilgiye ihtiyaç duyulması ve hesaplamalar için işlem süresinin artmasıdır. Ampirik batarya modeli doğru çıktılar verebilir, ancak modelin farklı senaryolar için doğrulanması gereklidir. ECM'ler, basit yapıları ve basit parametrelendirme süreçleri nedeniyle çeşitli endüstriyel uygulamalarda kullanılır. Ancak, modelin sadece test edildiği senaryolar için uygulanabileceği ve yaşlanma gibi süreçlerin entegre edilmesinin zor olduğu, bu nedenle uyarlama ve yeni veri toplamanın gerektiği unutulmamalıdır.

Üçüncü olarak, veri tabanlı batarya modelleme yöntemleri, büyük veri kümelerinden elde edilen bilgileri kullanarak batarya performansını ve kapasitesini tahmin etmeyi amaçlar. Bu modellerin artan popülaritesi, karmaşık doğrusal olmayan davranışları modelleme, adaptabilite ve yüksek doğruluk oranlarına sahip olmalarından kaynaklanmaktadır. Bu modeller, batarya ölçümlerinden oluşan bir veri kümesine dayanarak giriş parametreleri arasındaki ilişkiyi anlamak için makine öğrenme tekniklerini kullanır. Ancak, bu modellerin kullanımı dikkatli bir deneysel kurulum ve veri toplama sürecini gerektirir, çünkü yüksek kaliteli veri esastır. Kararsız verilerin kullanımı, modelin aşırı uyum sağlamasına veya tahminde bulunmasına neden olabilir.

Son olarak, bu tezde de detaylı olarak ele alınan Fizik Tabanlı Modeller, bataryadaki temel fiziksel ve kimyasal süreçleri matematiksel olarak ifade eder. Bu kategoriler, batarya davranışlarını analiz etmek ve tahmin etmek için farklı yöntemler sunar. Fizik tabanlı modellerden olan Tek Parçacık Modeli (SPM) ve Tek Parçacık Modeli ile Elektrolit (SPMe) gibi modeller, lityum iyonlarının bataryadaki hareketini ele alır. Bunlar, lityum iyonlarının katı parçacıklar içindeki hareketini hesaba katar. Doyle-Fuller-Newman (DFN) modeli ise lityum iyon bataryaların elektro-kimyasal davranışını detaylı bir şekilde simüle eder. Bu modeller, batarya performansını anlamak ve optimize etmek için kullanılır. Genellikle fizik tabanlı modelleme yöntemlerinde kullanılan bozulma modelleri, batarya ömrünü ve performansını artırmak için önemlidir. Çeşitli bozulma mekanizmalarını birleştirerek daha güvenilir ve uzun ömürlü batarya tasarımlarına katkı sağlarlar. Bu modeller, SEI büyümesi, lityum kaplama ve parçacık kırılması gibi bozulma süreçlerini simüle eder. Bu süreçler, bataryanın performansını olumsuz yönde etkiler ve dolayısıyla batarya tasarımında dikkate alınmalıdır. Sadece bataryada gerçekleşen elektriksel olayları kapsamakla kalmayıp aynı zamanda batarya performansını ciddi şekilde değiştiren önemli mikro ölçekli etkileşimleri de anlamak ve tanımlamak için elektrokimyasal model kullanılması önemlidir. Bu tarzda bir model, sistemin davranışını yüksek doğrulukla tanımlayabilir fakat birbirine bağlı birçok kısmi diferansiyel denklemin çözümlenmesi gerektiğinden çok fazla hesaplama yüküne sahiptir. Sonuç olarak, farklı batarya modelleri, farklı analizler için farklı yaklaşımlar sunar. Bu modellerin kullanılması, batarya teknolojisindeki ilerlemelerin ve daha verimli, daha güvenilir ve daha uzun ömürlü bataryaların geliştirilmesinin anahtarıdır.

Elektrikli araçlar için tasarım aşamasında batarya paketlerinin performans gereksinimlerini karşılayabilmesi için batarya ve yüklerin birlikte simülasyonu önemlidir. Büyük ölçekli batarya paketlerinin elektrikli araçlarda enerji depolama amacıyla kullanıldığı durumlarda bu özellikle önemlidir. Batarya talebini doğru bir şekilde tahmin edebilmek için çeşitli gerçek dünya kullanım senaryolarında simülasyonlar yapılmalıdır. Hibrit elektrikli araçlar için (HEV'ler) yapılan simülasyonlar içten yanmalı motorların, çoklu vitesli şanzımanların ve karmaşık hibrit karışım kontrol algoritmalarının dahil edilmesi nedeniyle oldukça karmaşıktır.Buna karşılık, yalnızca elektrikle çalışan araçlar (EV'ler) ve şarj edilebilir hibrit elektrikli araçlar (PHEV'ler) için yapılan simülasyonlar daha basittir. Genellikle içten yanmalı motorları ve tek hızlı sabit dişli sistemlerini içerirler. Elektrikli bir aracın simülasyonu için iki ana bileşen gereklidir; aracın kendisinin doğru bir tanımı ve aracın gerçekleştirmesi gereken işlev. Araç tanımı, batarya (hücre, modül, paket), motor, invertör (motor sürücü güç elektroniği), tahrik sistemi vb. hakkında detaylar içerir. Araç fonksiyonu, genellikle zamana karşı istenen bir hız profiline uyum sağlamayı içerir, genellikle bir "sürüş döngüsü" olarak adlandırılır. Elektrikli bir aracın simülasyonuna yaklaşım, optimum performans ve verimliliği sağlamak için dikkatli bir şekilde yapılmalıdır.

Bu çalışma, elektrikli araçlarda pil modelleme yöntemlerini kapsamlı bir şekilde incelemiş ve analiz etmiştir. Farklı kimyasal bileşimlere sahip piller için çeşitli fizik tabanlı modelleme yöntemlerinin performansları detaylı olarak araştırılmış ve karşılaştırılmıştır. Bu modellerin karmaşıklıkları ve tahmin yetenekleri, literatürdeki çalışmalar ışığında özetlenmiş ve değerlendirilmiştir. Araştırmada ilk olarak tüm batarya modelleme yöntemleri kapsamlı bir şekilde incelenmiştir. Daha sonra, farklı kimyasal bileşimlere sahip piller için fizik tabanlı modelleme yöntemleri ayrıntılı olarak simüle edilmiş ve analiz edilmiştir. Bazı parametrelerin literatürdeki değerlerinin doğruluğundan emin olunmadığından dolayı, daha verimli değerler elde etmek için optimizasyon çalışmaları yapılmıştır. Bir elektrikli araç modeli oluşturmak için gerekli tüm matematiksel formüller ele alınmış ve simülasyon ortamları kullanılarak elektrikli araç modeli geliştirilmiştir. Elektrikli araç modeli, batarya boyutlandırma ve yol mesafesi hesaplama çalışmalarında kullanılmak üzere fizik tabanlı modelleme yöntemleriyle entegre edilmiştir. Araç modeli ve pil modelleme yöntemleri kullanılarak detaylı bir simülasyon çalışması gerçekleştirilmiştir. Simülasyonun doğruluğunu test etmek için mevcut simulasyon sonuçları ile daha önce literatürde gerçekleştirilen menzil verileri karşılaştırılmıştır. Hücrenin yaşlanmasına etki edebilecek bazı yöntemler detaylı olarak incelenmiş ve bu değişiklikler çevrimlerde gözlemlenmiştir. Sonuç olarak bu çalışma, elektrikli araçlarda pil modelleme yöntemleri için kapsamlı bir analiz sunmuştur. Farklı kimyasal bileşimlere sahip piller için modelleme yöntemlerinin performanslarını karşılaştırarak ve mevcut modelleme tekniklerini optimize ederek, elektrikli araçlarda pil performansının daha doğru ve güvenilir bir şekilde tahmin edilmesine yardımcı olmuştur. Bu sayede, pil ömrünün uzatılması ve elektrikli araçların daha sürdürülebilir hale getirilmesi için önemli bir adım atılmıştır.

Çalışmanın önemi ve literatüre katkıları ise, batarya modelleme yöntemleri hakkında güncel ve kapsamlı bir bilgi kaynağı sunmuştur. Farklı kimyasal bileşimlere sahip piller için pil modelleme yöntemlerinin performanslarını karşılaştıran kapsamlı çalışmalardan biridir. Farklı kimyasal bileşimlere sahip piller için en uygun modelleme yöntemlerini belirlemede yardımcı olmuştur. Mevcut pil modelleme tekniklerini optimize ederek pil performansının daha doğru tahmin edilmesine yardımcı olmuştur. Elektrikli araç tasarımı ve optimizasyonu için yeni fikirler ve araçlar sunmuştur ve elektrikli araçlarda pil ömrünün uzatılmasını içeren bilgilerle daha sürdürülebilir bir geleceğe katkıda bulunmuştur.

1. INTRODUCTION

With the widespread adoption of electric vehicles, lithium-ion batteries have emerged as a fundamental technological solution in the automotive industry with their high energy density and fast charging capabilities. Continuously evolving lithium-ion battery technology has a crucial role in the transformation of the automotive industry, targeting important goals including increasing the range of electric vehicles, reducing charging times and improving [4]. After this breakthrough in electric vehicles and lithium-ion batteries, it has become increasingly important to make accurate modeling, predictions and calculations on both the vehicles and the batteries. Therefore, several modeling techniques have been investigated. In this chapter, we will review electric vehicles, lithium-ion batteries and their modeling techniques.

1.1 Purpose of Thesis

The main goal of the thesis is to first examine which physics-based modeling method performs better for which chemistry by experimenting with different physics-based modeling methods for different chemistries, to establish a simulation environment for BEVs, to simulate the battery using vehicle and physics-based modeling methods in this simulation environment, to examine battery performance and characterization, and to predict the range of the vehicle.

Main highlights and contributions of the thesis:

1. Summarized and compared various modeling methods in existing literature based on their complexity and outcomes.

2. Explored the relationship between these modeling methods and specific chemistries, aiming to discern which methods are more suitable for particular chemical systems.

3. Updated modeling approaches with optimization methods to enhance accuracy, and investigated which chemistries are better suited for physics-based modeling understand.

4. Building a simulation environment for an electric vehicle in python and integrating it with different physics-based battery models in python for BEV simulation allows to take the driving profile, grade and ambient temperature as an input and provide battery states voltage, SOC etc. as an output.

1.2 Literature Review

There are many advantages to electric vehicles (EVs) that have been contributing to their growing popularity and worldwide acceptance. According to a report by the International Energy Agency (IEA), one of the most important advantages for electric vehicles is its environmental effects. With making the dependence on fossil fuels and emitting fewer greenhouse gases very limited and minimum during operation compared to vehicles with conventional internal combustion engines, EVs to have an very critical role to play in reducing the climate change and in improving air life and quality [5]. Also, EVs bring many economic benefits for both consumers and the society as a collective. Although the first purchasing price for EVs can be higher than for traditional vehicles, studies demonstrate that electric vehicle owners can benefit by lower operating and maintenance costs across the vehicle's lifetime. [6]. In parallel, government funding like tax credits, rebates and subsidies encourage consumers to adopt EVs, can boost further enhancing their marketability and attractiveness [5]. However along with these benefits, EVs do face several key challenges that are hindering their wide acceptance. Limited driving range of EVs compared to conventional vehicles is one of the key challange. Despite lots of advances available in battery technology, range anxiety still remains a very big concern for many consumers, especially for long-distance travellers [7]. Furthermore, the another important and critical challenge is availability and accessibility of charging infrastructure. While the number of charging stations has increased globally, uneven distribution and lack of standardized charging protocols prevent convenient and widespread adoption of charging technology [8]. Furthermore, the initial cost of EVs remains a barrier for many potential buyers particularly where EV promotions are limited or not even exist [6]. The environmental impact with battery production and disposal raises concerns about the overall sustainability of EVs. Although EVs produce fewer emissions during operation, the environmental footprint of battery production and recycling processes must be addressed to ensure the long-term sustainability of electric mobility [9]. Addressing these challenges requires concerted efforts from governments, industries and stakeholders to stimulate technological innovation, improve infrastructure and support policies that accelerate the transition to electric mobility while still maintaining the environmental sustainability.

The roots of electric vehicles begin with the invention of the electric motor. The electric motor, developed by Michael Faraday in the early 19th century, formed the basis of electric vehicles. But the first commercially produced electric vehicles appeared in England and France in the middle 1830s. These vehicles were mainly public transportation vehicles like trams and trolleybuses, which are mostly used in rail systems. In the 1880s, electric vehicles popularity increased a lot, especially in urban transportation. In major US cities such as New York and Chicago, streetcars have evolved into electric vehicles that transport people more efficiently. Electric taxis also began to be widely used during this same period. Electric vehicles were preferred since they are both quiet and environmentally friendly. However, with the development of internal combustion engines and the spread of cheap oil in the early 20th century, electric vehicles remained relatively in the background. Gasoline vehicles have become more attractive than electric vehicles and provide advantages such as longer range and faster refill time. During this period, electric vehicles were mostly used as small vehicles for private use but did not play a significant role in the public transportation and commercial vehicle segments. Throughout the 20th century, electric vehicles have faced technical and infrastructural challenges such as limited range, high cost, and lack of charging infrastructure. However, in recent years, electric vehicles have begun to gain popularity again. Increasing environmental concerns, the need for energy independence and advances in technology have brought electric vehicles back to the agenda. Later, significant technological advances were made towards electric vehicles in the early 21st century. In particular, advances in battery technology have increased the range of electric vehicles and shortened their charging times. In addition, under the leadership of leading companies such as Tesla, electric vehicle manufacturers have also developed more efficient and attractive models. These developments have enabled electric vehicles to become widespread. Today, many countries are implementing various policies and incentives to promote electric vehicles. These policies include measures such as purchasing subsidies, tax reductions, expansion of charging infrastructure and promotion of renewable energy sources. However, there are still some obstacles to widespread adoption of electric vehicles; especially inadequate charging infrastructure, high costs and range concerns. [10].

With the coming to the fore of electric vehicles and renewable energy storage systems, the development of battery technology has also gained great momentum. This development has gone through various stages from past to present. The roots of battery technology date back to the 18th century. The voltaic cell, invented by Alessandro Volta, laid the foundation for electrochemical cells. This invention laid the foundations of modern battery technology. The Daniell Cell, later developed by John Frederic Daniell in the mid-19th century, went one step further and provided a more stable voltage. At that time, battery technology was still immature and faced many limitations. At the turn of the century, Thomas Edison's lead-acid battery found application in the first electric vehicles. However, at that time, battery technology was still very limited and faced significant problems in terms of efficiency. However, the World War II era led to the rapid development of battery technology. The increased demand for battery-based technologies during the war accelerated research and development efforts. New types of batteries emerged in the post-war period, such as nickel-cadmium and nickel-metal hydride. These batteries provided more efficient power sources for portable devices. But perhaps the most important turning point came with the commercial launch of lithium-ion batteries. Lithium-ion batteries have a wide range of applications, from electronic devices to electric vehicles, due to their advantages such as high energy density, light weight and low discharge rate. These batteries were commercially released by Sony in 1991 and have been continuously improved since then, becoming a major force in the electric vehicle industry. Today, battery technology is developing rapidly and more efficient, safer and more environmentally friendly battery systems are constantly being developed. Researchers are working on the next generation of batteries with features such as higher energy storage capacity, faster charging times and longer life. These developments are helping to speed up the energy transformation worldwide, leading to broader adoption of electric vehicles and renewable energy storage systems [11].

In a world where electric vehicles are becoming so important, electric vehicle batteries and batteries used in all other electronic devices continue to become more significant.In today's world, importance of the batteries, which are energy storage systems used in almost all electronic devices in our lives, ranging from electric vehicles to consumer electronics, medical devices, industrial applications, aerospace, and defence, is increasing every day. Batteries are devices that store and provide electrical energy through reversible chemical reactions. Whilst batteries with various chemistries are used today, the most popular type of battery is lithium-ion batteries. Lithium-ion batteries are widely used in electric vehicles, consumer electronics, and energy storage systems since they have high energy density, low self-discharge, and are lightweight. They are available in various chemistries such as Lithium Cobalt Oxide (LiCoO2), Lithium Iron Phosphate (LiFePO4), and Lithium Nickel Manganese Cobalt Oxide (NMC). The increasing importance of these batteries has always been directly linked to the effective use of their capabilities. Achieving this level of efficiency and usefulness required the development of precise and feasible battery models.

The emergence of lithium-ion (Li-ion) batteries has heralded a new era in portable electronics, renewable energy storage, and especially vehicle electrification. However, despite their transformative potential, li-ion batteries face many challenges that require sustained effort and innovative solutions. Safety, which is a critical element in the widespread adoption of Li-ion technology, is one of the most important of these challenges. [12]. Especially in cases of damage or overcharging, the risk of thermal runaway creates safety hazards like fire and explosion. Researchers have been carefully working to develop safer electrolytes and materials to minimize these risks and ensure the reliability of Li-ion batteries in various applications. The energy density is another major challenge, in particular in the field of electric vehicles [13]. With the automotive industry moving towards electrification, the capacity of Li-ion batteries to efficiently store and transmit energy is of crucial importance. Not only does improved energy density extend the range of electric vehicles, it also reduces the weight and size of batteries, therefore improving and optimizing the overall vehicle performance and the driving experience. However, the quest for higher energy density still needs to contend with the problem of sustained cost [14].Dependence on materials such as cobalt and complex manufacturing processes contribute to the high cost of Li-ion batteries. Addressing cost concerns is imperative to further accelerate the transition to sustainable transport solutions and democratize access to electric vehicles. Furthermore, the longevity of Li-ion batteries, characterized by cycle life, remains an important area of focus [13]. The degradation in battery performance with time, as reflected by reduced capacity and lifetime, presents challenges for both consumer electronics and electric vehicles. Strategies aimed at extending cycle life through improved battery management systems and robust electrode materials are required to improve the durability and reliability of Li-ion batteries. Within the broader context of environmental sustainability [12], Li-ion battery technology has been under scrutiny for its environmental footprint. The life cycle of Li-ion batteries, which spans sourcing to end-of-life disposal, has environmental impacts that require careful management. Consistent sustainable practices, including responsible sourcing of materials and efficient recycling processes, are integral to mitigating these environmental concerns and ensuring the long-term viability of Li-ion technology. Li-ion battery challenges highlight the importance of continued research and innovation in the field of energy storage. With the automotive industry transitioning towards electrification, the role of Li-ion batteries in powering electric vehicles is becoming critical. Li-ion technology's continued development, supported by safety, energy density, cost-effectiveness, longevity and environmental sustainability, is essential to achieving a cleaner and greener transportation future.

1.3 Hypothesis

The thesis is outlined as follows:

- Battery modeling approaches need to be investigated in order to compare the models. Chapter 2 describes the models used in this thesis. It also describes the degradation modeling that is investigated in this work.

- In Chapter 3, the vehicle model that is needed for range estimation and the vehicle and battery simulation environment is explained.

- In Chapter 4, the electrochemical models described in Chapter 2 and different chemistries are compared, in addition, a BEV model is created by integrating the vehicle model described in Chapter 3 and the behavior of the battery is analyzed under specific cycles and range comparisons are carried out.

2. ELECTROCHEMICAL BATTERY MODELS

Electrochemical battery modeling methods cover a wide range of techniques developed to optimize the performance, lifetime and safety of batteries. They are used in the design, simulation and analysis of battery systems, contributing significantly to the development of energy storage technologies. These models can help to understand and control the physical and chemical processes of batteries, so that more efficient, reliable and long-lasting battery systems can be designed.

In this chapter, different types of electrochemical battery modeling methods and their application areas are covered. Physical models represent the internal structure and chemical processes of batteries in detail, while empirical models predict the behavior of the battery with relationships derived from experimental data. Furthermore, data-based models use machine learning and artificial intelligence techniques to extract meaningful patterns from large data sets and predict the future performance of the battery.

The study of modeling methods plays a key role in the development of battery technologies. These methods enable the improvement of important parameters such as battery design and optimization, energy density, charge-discharge cycle life and safety. Understanding and applying electrochemical battery modeling methods is an important step towards achieving sustainable energy solutions.

2.1 Modelling Approaches for Lithium-Ion Batteries

In literature, battery models are categorized into four main groups [15]. The classical empirical models, based on experiments, include the Shepherd model [16], the Unnewehr universal model [16,17], and the Nernst model [18]. The Nernst model is noted for its accuracy, while the Shepherd model is particularly effective for continuous discharge currents. Enhancements to these models involve adding more parameters and variables. For example, improving the Nernst model's prediction of dynamic terminal voltage is possible by incorporating two constants ($\tau 1$ and $\tau 2$) [19]. Additionally, refining the Nernst model with the hysteresis effect offers further improvements [20]. However, such enhancements increase computational complexity. The accuracy of these three models in predicting terminal voltage is compared in [21].

Secondly, the Equivalent Circuit Model (ECM) contains a SOC-dependent voltage source, an internal resistor and Resistance-Capacitance (RC) pairs that describe the electrical relationship between the inputs (current, SOC and temperature) and the terminal voltage [22]. Figure 2.1 illustrates a schematic of a part of a simple electrical circuit that contains resistors (R_0 and R_1) and a capacitor (C). The model comprising an internal resistor and a resistor-capacitor block between the open circuit voltage and the terminal voltage is used as a common battery model [23]. When contrasting ECMs with empirical models, it becomes evident that ECMs exhibit a high degree of simplification in their ability to accurately discern the electrical properties inherent to batteries. Besides, because of the large number of circuit components and their variations, the ECM gives researchers enough flexibility to design a structure appropriate for their application. By adding more elements, the model can yield more correct and precise simulations of battery behavior. The disadvantage of using more elements in the equivalent circuit is that more information about the cell is needed for parameterization and CPU time for calculations increases [24]. The empirical battery model can give accurate outputs, but the model requires validation for all different scenarios. ECMs are used for various industrial applications due to their simple structure and simple parameterization process. But the model can only be applied to the scenarios for which it has been tested and processes such as ageing are difficult to incorporate, so adaptation and new data collection are required [25].

Data-driven battery modeling methods aim to predict battery performance and capacity using information derived from large datasets. Their increasing popularity stems from their ability to model complex nonlinear behaviors, adaptability, and high accuracy rates. These models employ machine learning algorithms to understand the connection between input parameters like voltage, temperature, current, and output parameters like state of charge and capacity, based on a dataset of battery measurements. However, the use of these models requires a careful experimental setup and data collection

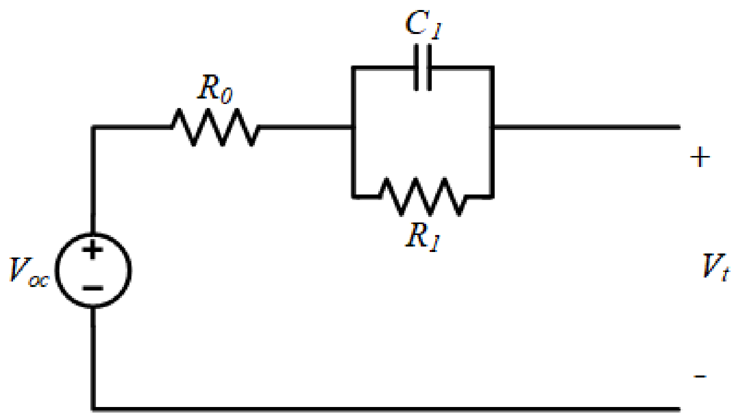

Figure 2.1 : Equivalent circuit model (ECM)

process, as high-quality data is essential. The use of unstable data can lead to the model overfitting or underpredicting [26,27]. Physics-based models, also known as electrochemical models, mathematically express the fundamental physical and chemical processes in batteries, including electrochemical reactions, ion transport, electron flow, and the materials' thermodynamic and kinetic properties. Lithium ion battery cell flow among the solid and electrolyte phases is oftentimes involved in these models, along with charge and mass conservation in both phases. The electrochemical model is represented in the form of nonlinear Partial Differential Equations (PDEs). For this reason, a pre-condition for utilizing an electrochemical model to derive a direct analytical solution is to turn the PDEs into Ordinary Differential Equations (ODEs). Numerical techniques like integral approximation, Pade approximation, Ritz method, finite element method and finite difference methods which are mostly preferred in order to making nonlinear PDEs discretize in electrochemical battery models [28,29]. Employing these models enables accurate predictions of battery performance under various conditions, including charge-discharge cycles, temperature variations, and aging effects. There are many electrochemical models in the literature; these offer various approaches to understanding the complex internal structure and operational mechanisms of batteries. Electrochemical battery modeling comprehensively addresses the electrochemical reactions of the battery, thermal management, electrical characteristics, and aging processes. These models provide insights into how batteries will perform under real-world conditions, assisting in the development of design and operational strategies necessary to make batteries more efficient and longer-lasting. In [30], it was first used to determine the parameters that extract the model of the LFP cell, presents simulations of power and capacity degradation of LiFePO4-Graphite Li-ion batteries by simplifying the electrochemical and thermal aging model. They developed a model to understand how the performance of LFP cells changes with time. The model simulates the degradation in the capacity and power of the battery, taking into account thermal as well as electrochemical interactions. This study can be considered as an important step towards understanding the aging processes of LiFePO4-Graphite Li-ion batteries and improving their performance. Since other modeling attempts using the parameters presented in the article, [30], did not give the desired modeling results, an additional study, [31], has been carried out in 2021 in order to optimize the parameters and to find variations and parameters that produce more accurate results.

Focusing on the lithium polymer battery cell, a method for determining the electrochemical model of a lithium-ion battery is introduced [32,33]. For the development of a comprehensive model including electrochemical and thermal properties as well as material properties, a series of experiments and analyses were carried out. First of all, several chemical experiments were conducted to determine the electrochemical properties of the lithium-ion battery. These experiments were performed to determine the material properties of the electrodes, the diffusion rates of lithium ions and the electrochemical reaction kinetics. Then, physical experiments were performed to determine the material properties and thermal behavior. These experiments were carried out to evaluate the conductivity properties of the electrode materials, temperature profiles and thermal conductivities of the lithium-ion battery. The data obtained were used to determine the parameters of the electrochemical model used to simulate the behavior of the battery. This study contributes to more accurate modeling of lithium-ion batteries and a better understanding of their performance. In addition to this model, some of the parameters used in the study, which mostly will be discussed later, are tab placement parameters taken from measurements in [34] and some electrode and electrolyte properties from [35]. With a focus on the lithium-cobalt oxide-graphite cell, an electrochemical, thermal and mechanical model is described that explores the non-uniform stress distribution in lithium-ion pouch cells [35]. The model adopts a pseudo-2D approach involving mechanically coupled diffusion physics, which enables the study of the stress response in electrode particles. The results obtained in the study indicate that the model can successfully predict voltage, temperature and thickness variations in pouch cells and are in agreement with experimental data.

To implement all these modeling techniques and to ensure the low risk and longer useful life of the lithium ion battery for its better operation, there is an important and cruical need for a battery management system (BMS). The battery management system should be able to provide prediction without any error to the SOC, state of battery completeness and remaining useful life remaining in the cell. Estimating the state of charge of the battery is one of the most important features of BMS tasks. Yet the SOC is very hard to predict accurately. Reason for that is the SOC is the inside states of the battery cell and can be observed and measured directly. Therefore, the SOC must be calculated roughly. Until now, several tehniques of estimating the SOC of the battery are presented, which are generally separated by two groups: free model and model-based. Free models include Ampere-hour (Ah) or coulomb count, open circuit voltage (OCV). Apart from these two methods, the development reported in [36] is the method that applies a particle filter modified with the RLS algorithm to improve the accuracy of predicting the SOC of a lithium-ion battery in electric vehicles. The results show that the proposed method works effectively compared to other methods. The following are the details for the 3 main categories most commonly found in the literature, but another similar approach is the Two-parameter approximation model, Single Particle Model (SPM) and Decoupled Solution Approach, which are also grouped into 3 main categories. Aging studies related to this classification were also performed for Lithium Manganese Oxide (LMO) cell and it was concluded that for the same electrolyte and cell parameters, the simulation methods can be applied to any cell chemistry [37].

2.2 Single Particle Model (SPM)

Electrochemical battery models play a key role in understanding energy storage and conversion processes. These models typically incorporate a mix of electrochemical interactions, transport events and circuit elements to truly describe the complex behavior of batteries. The electrochemical model of mechanism can not only define macroscopic physical quantities like voltage and current, but also simulate important microscopic physical parameters inside the cell, which is appropriate for use in the degradation examinations and aging explores of cell behavior [38].

Physics-based models provide a deeper comprehension through directly involving the electrochemical reactions and transport phenomena underlying the battery. Frequently, such models rely on partial differential equations (PDEs) to describe the species concentration, charge and temperature distributions in the battery. The physics-based models, while more complex and computationally intensive compared to lumped-parameter models, offer higher accuracy and can capture nuances such as temperature effects, electrolyte transport limitations and electrode degradation. There are also hybrid approaches that combine aspects of both granular parameter and physics-based models, aiming to strike a balance between computational efficiency and accuracy. Consequently, the model choice depends on the specific application requirements, the level of detail needed and the computational resources available.

As a representation of a Li-ion battery, the Single Particle Model (SPM) accounts for the transport of lithium ions within the solid particles of the battery electrodes. As the model assumes a constant concentration of lithium ions in the electrolyte and ignores the diffusion of the electrode concentration along the electrode. Diffusion within each electrode is ruled by Fick's law in the spherical orientation. Boundary conditions at the surface and core of the particle are defined to represent the intercalation-deintercalation process of lithium ions. The molar flux at the surface is influenced by the input current density and the diffusion rate constant. The Butler-Volmer equation considers the electrode concentration to be equal to the electrolyte concentration and associates the overpotential at the solid-electrolyte interface with the current density. Negative and

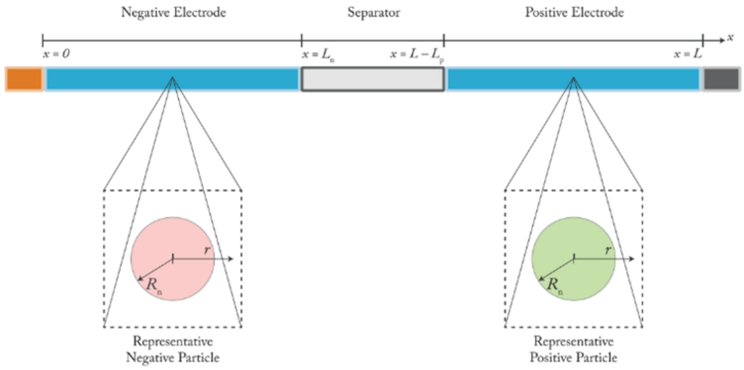

Figure 2.2 : SPM representation of Lithium-Ion batteries [1].

positive phase overpotentials are expressed as functions of temperature, charge transfer coefficient and electrode surface area. The exchange current density is calculated based on the constant electrolyte concentration and the maximum concentration of the electrode. The state of charge (SoC) of the battery can be determined using normalized lithium concentrations on the surface of the electrodes. The total cell potential takes into account contributions from the overpotentials of the electrodes and open circuit potential functions [32,33].

More detailed explanation of SPM and its formulas, SPM comprises of two diffusion equations that exhibit spherical symmetry: one operating within a typical negative particle ($k = n$) and the other within a typical positive particle ($k = p$). At the core of each particle, the standard no-flux condition is enforced. Given the SPM's assumption that all particles within an electrode exhibit identical behavior, the flux at the particle surface equates to the current (I) divided by the electrode thickness (L_k). The concentration of lithium within electrode (k) is represented as (c_k). The model equations governing the SPM are as follows eqs. (2.1) to (2.4) [39,40]:

$$\frac{\partial_{c_{s,k}}}{\partial_t} = -\frac{1}{r_k^2}\frac{\partial}{\partial_{r_k}}(r_k^2 N_{s,k}) \tag{2.1}$$

$$N_{s,k} = -D_{s,k}\left(c_{s,k}\right)\frac{\partial_{c_{s,k}}}{\partial_{r_k}}, \qquad k \in n, p \tag{2.2}$$

$$
\begin{aligned}
N_{s,k}\big|_{r_k=0} &= 0, \qquad k \in n, p, \\
N_{s,k}\big|_{r_k=1} &= \begin{cases} \frac{1}{F_{a_n} L_n}, & k = n \\ -\frac{1}{F_{a_p} L_p}, & k = p \end{cases}
\end{aligned} \tag{2.3}
$$

$$
c_{s,k}(r_k, 0) = c_{s,k,0}, \qquad k \in n, p \tag{2.4}
$$

where $D_(s,k)$ is the diffusion coefficient in the solid, $N_(s,k)$ denotes the flux of lithium ions in the solid particle within the region k, and r_k is the radial coordinate of the particle in electrode k. The voltage is obtained from the expression in eq. (2.5):

$$
\begin{aligned}
V = \; & U_p(c_p)\,|_{r_p=1} - U_n(c_n)\,|_{r_n=1} \\
& - \frac{2RT}{F} sinh^{-1}\left(\frac{I}{2 j_{0,p} a_p L_p}\right) \\
& - \frac{2RT}{F} sinh^{-1}\left(\frac{I}{2 j_{0,n} a_n L_n}\right)
\end{aligned} \tag{2.5}
$$

with the exchange current densities given by in eq. (2.6),

$$
j_{0,k} = (c_k)^{1/2}(1 - c_k)^{1/2} \tag{2.6}
$$

2.3 Single Particle Model with Electrolyte (SPMe)

Single Particle Model with Electrolyte Dynamics (SPMe) extends the Single Particle Model (SPM) to cover electrolyte diffusion dynamics across the length of battery electrodes. It presents diffusion equations for the negative electrolyte, separator and positive electrolyte, taking into account electrolyte polarization and conductivity due to overpotential. The diffusion equations rule the electrolyte diffusion through the thickness of the electrodes and separator, with additional terms which represent the electrolyte polarization and conductivity. Boundary conditions provide stability of concentration at the interfaces between the different regions. The electrolyte potential is divided into electrolyte overpotentials that rely on conductivity and electrolyte polarization. Depends on the electrolyte conductivity concentration and is derived from experimental data. A function of the lithium concentration and the volume fractions of each zone is defined taking into account the porous nature of the electrolyte medium. The Bruggman correction helps to determine the effective conductivity and the Bruggman exponent measures the effect the porous medium has on the electrolyte properties. Higher Bruggman constants result in lower effective conductivity, directly affecting the cell voltage. Electrolyte electrical overpotential due to electrolyte conductivity is represented as ohmic resistance considering the current density and the thicknesses of the electrodes and separator. It is identified by electrochemical impedance spectroscopy. The electrical overpotential due to lithium-ion diffusion is calculated according to the electrolyte activity coefficient, that considers the effects of electrolyte concentration and temperature. In this case, the activity coefficient is calculated separately for each phase. Last but not least, it is calculated as the sum of the solid phase potential (from the SPM) and the electric overpotential that are caused by electrolyte conductivity and polarization. Overall, SPMe provides a more comprehensive understanding of battery behavior by integrating electrolyte dynamics and their effect on cell performance and voltage. More detailed explanation of SPMe and its formulas, SPMe encompasses equations governing the lithium concentration within representative particles situated in the negative electrode $(c_{s,n})$ and the positive electrode $(c_{s,p})$, alongside an equation dictating the behavior of the first-order correction to the lithium concentration within the electrolyte $(c_{e,k})$, where a Roman subscript $k \in n, s, p$ designates the negative electrode, separator, and positive electrode regions, respectively. Adhering to the standard practice, the no-flux condition is enforced at the center of each particle, and the flux at the particle's surface is determined as the ratio of the current (I) to the thickness of the respective electrode (L_k), akin to the SPM. Given the transfer of lithium between the electrolyte and particles, the flux through the particle's surface is incorporated into the electrolyte diffusion equation as a source/sink term. Notably, there's no lithium transfer between the electrolyte and current collectors, resulting in no-flux boundary conditions on the lithium concentration within the electrolyte $(c_{e,k})$ at either end of the cell. It is imperative to set initial conditions reflecting the establishment of an initial concentration within each particle $(c_{s,k}(t=0) = c_{s,k,0})$, and ensuring no deviation from the initial (uniform) lithium concentration within the electrolyte $(c_{e,k}(t=0) = c_{e,0})$ [23, 24]: Particles formulas are given in eqs. (2.7) to (2.13) where

$D_{s,k}$ is the diffusion coefficient in the solid, $N_{s,k}$ denotes the flux of lithium ions in the solid particle within the region k, and r_k is the radial coordinate of the particle in electrode k.

$$\frac{\partial_{c_{s,k}}}{\partial_t} = -\frac{1}{r_k^2}\frac{\partial}{\partial_{r_k}}(r_k^2 N_{s,k}), \tag{2.7}$$

$$N_{s,k} = -D_{s,k}\left(c_{s,k}\right)\frac{\partial_{c_{s,k}}}{\partial_{r_k}}, \qquad k \in n,p, \tag{2.8}$$

$$\begin{aligned} N_{s,k}\big|_{r_k=0} &= 0, \quad k \in n,p, \\ N_{s,k}\big|_{r_k=1} &= \begin{cases} \frac{1}{F_{a_n}L_n}, & k=n, \\ -\frac{1}{F_{a_p}L_p}, & k=p, \end{cases} \end{aligned} \tag{2.9}$$

$$\varepsilon_k \frac{\partial_{c_{e,k}}}{\partial_t} = -\frac{\partial N_{e,k}}{\partial x} + \begin{cases} \frac{1}{FL_n}, & k=n \\ 0, & k=s \\ \frac{1}{FL_p}, & k=p \end{cases} \tag{2.10}$$

$$\begin{aligned} N_{e,k} = -\varepsilon_k^b D_e \frac{\partial_{c_{e,k}}}{\partial x} + \\ \begin{cases} \frac{xt+IRT}{FL_n}, k=n \\ \frac{t+IRT}{F}, k=s \\ \frac{(1-x)t+IRT}{FL_p}, k=p \end{cases} \end{aligned} \tag{2.11}$$

$$N_{e,n}|_{x=0} = 0,\ N_{e,p}|_{x=L} = 0 \tag{2.12}$$

$$c_{e,k}(x,0) = 0, \quad k \in n,s,p \tag{2.13}$$

Voltage formulas are given in eqs. (2.14) to (2.22) where U_k is the reference OCP, b is the Bruggeman coefficient, j is the exchange-current density, ϕ is the electric potentials, F is the Faraday's constant, R is the universal gas constant and T is the temperature, L_n,L_s,L_p are the thicknesses of the negative electrode, separator, and positive electrode respectively.

$$V = U_{eq} + \eta_r + \eta_c + \Delta\Phi_{Elec} + \Delta\Phi_{Solid} \tag{2.14}$$

$$U_{eq} = U_p(c_p)|_{r_p=1} - U_n(c_n)|_{r_n=1}, \tag{2.15}$$

$$\eta_r = -2\sinh^{-1}(\frac{I}{\bar{j}_{0,p}L_p}) - 2\sinh^{-1}\left(\frac{I}{\bar{j}_{0,n}L_n}\right) \tag{2.16}$$

$$\eta_c = 2\left(1-t^+\right)\frac{RT}{F}\left(\bar{c}_{e,p} - \bar{c}_{e,n}\right) \tag{2.17}$$

$$\bar{j}_{0,n} = \frac{1}{L_n}\int_0^{L_n} \frac{\gamma_n}{C_{r,n}}(c_n)^{1/2}(1-c_n)^{1/2}(1+C_e c_{e,n})^{1/2}dx \tag{2.18}$$

$$\bar{j}_{0,p} = \frac{1}{L_p}\int_{1-L_p}^{L_p} \frac{\gamma_p}{C_{r,p}}(c_p)^{1/2}(1-c_p)^{1/2}(1+C_e c_{e,p})^{1/2}dx \tag{2.19}$$

$$\Delta\Phi_{Elec} = -\frac{C_e I}{\gamma_e \kappa_e(1)}\left(\frac{L_n}{3\varepsilon_n^b} + \frac{L_s}{\varepsilon_s^b} + \frac{L_n}{3\varepsilon_p^b}\right) \tag{2.20}$$

$$\Delta\Phi_{Solid} = -\frac{I}{3}(\frac{Lp}{\sigma_p} + \frac{L_n}{\sigma_n}) \tag{2.21}$$

$$\bar{c}_{e,n} = \frac{1}{L_n}\int_0^{L_n} c_{e,n}dx, \ \bar{c}_{e,p} = \frac{1}{L_p}\int_{L-L_p}^{L_n} c_{e,p}dx \tag{2.22}$$

2.4 Doyle-Fuller-Newman (DFN)

The Doyle-Fuller-Newman (DFN) model introduced and developed by Doyle and Newman is a widely used electrochemical model for simulating the operation of lithium-ion batteries. It integrates mass transfer, diffusion, migration and reaction kinetics to provide a comprehensive understanding of battery behavior. The DFN model is acknowledged as the most widespread and extensively verified model in the literature for investigating Li-ion batteries. It is made up of equations describing the movement of lithium ions within the battery electrodes and electrolyte. These equations are essentially based on partial differential equations (PDEs) governing diffusion phenomena. In particular, diffusion PDEs in solid particles are very crucial in the DFN model. They provide significant information about the presence of lithium ions for electrochemical reactions and the lithium concentration within the electrodes. However, resolving these solid phase diffusion equations needs more computational work compared to the electrolyte phase diffusion equations. This is mainly because solid phase diffusion changes not only through the thickness of the electrode on the macroscopic scale (x-scale), but also through the radius of the particles on the microscopic scale (r-scale). The DFN model is composed of coupled PDAEs, and some of the parameters in these equations are coupled together such that it is mathematically not possible to determine all parameter values correctly and uniquely from input–output data [41]. Exact parameterization is difficult as many of the required quantities must be inferred indirectly from experimental data. Moreover, there can be significant variability from device to device, even in cells that are seemingly prepared in the same way. Therefore, proper parameterization is an obstacle that must be addressed to obtain the maximum benefit from DFN models [42]. Due to the computational complexity of solid phase diffusion, efforts are being made to simplify these equations to allow for real-time simulation capabilities. This simplification is very important for practical applications where rapid prediction of battery performance is necessary [43]. Overall, the DFN model is a strong tool for investigating the electrochemical behavior of Li-ion batteries and offers insights into the various processes that occur within the battery during charge-discharge cycles. More detailed explanation of DFN and its formulas, DFN model encapsulates equations ensuring the conservation of charge and mass within both the solid and electrolyte phases, while also outlining the behavior governing electrochemical reactions transpiring at the interface between the solid and electrolyte [2,44]. A Roman subscript is employed to signify the negative electrode, separator, and positive electrode regions, respectively. The model equations for the DFN are as follows [39,40,45]: Charge conservation formulas are given in eqs. (2.23) to (2.25) where a_k is the electrode surface area density, ε_k is the electrolyte volume fraction, c_e is the lithium-ion concentration in electrolyte, a_k is the electrode surface area density, i is the current densities.

$$\frac{\partial i_{e,k}}{\partial x} = \begin{cases} a_k j_k, & k = n, p \\ 0, & k = s \end{cases} \tag{2.23}$$

$$i_{e,k} = \varepsilon_k^b K_e\left(c_{e,k}\right)\left(-\frac{\partial \phi_{e,k}}{\partial x} + 2(1- \ t^+)\frac{RT\partial}{F\partial x}\left(\log\left(c_{e,k}\right)\right)\right), \qquad k \in n,s,p \tag{2.24}$$

$$I - i_{e,k} = -\sigma_k \frac{\partial \phi_{e,k}}{\partial x}, \quad k \in n,s,p \tag{2.25}$$

Mass conservation formulas are given in eqs. (2.26) to (2.29) where N is the molar fluxes and D_e is the electrode diffusivity.

$$\varepsilon_k \frac{\partial c_{e,k}}{\partial t} = -\frac{\partial N_{e,k}}{\partial x} + \frac{1}{F}\frac{\partial i_{e,k}}{\partial x}, \qquad k \in n,s,p \tag{2.26}$$

$$N_{e,k} = \varepsilon_k^b D_e\left(c_{e,k}\right)\frac{\partial c_{e,k}}{\partial x} + \frac{t^+}{F} i_{e,k}, \qquad k \in n,s,p \tag{2.27}$$

$$\frac{\partial c_{s,k}}{\partial t} = -\frac{1}{r_k^2}\frac{\partial}{\partial_{r_k}}\left(r_k^2 N_{s,k}\right), \qquad k \in n,p \tag{2.28}$$

$$N_{s,k} = -D_{s,k}\left(c_{s,k}\right)\frac{\partial_{c_{s,k}}}{\partial_{r_k}}, \qquad k \in n,p. \tag{2.29}$$

Electrochemical reactions formulas are given in eqs. (2.30) to (2.32).

$$j_k = 2 j_{0,k} \sinh\left(\frac{F\eta_k}{2RT}\right), \qquad k \in n,p, \tag{2.30}$$

$$j_{0,k} = {c_{s,k}}^{\frac{1}{2}}\left(1 - c_{s,k}\right)^{\frac{1}{2}} {c_{e,k}}^{\frac{1}{2}}|_{r_k=1}, \qquad k \in n,p, \tag{2.31}$$

$$\eta_k = \phi_{S,k} - \phi_{e,k} - U_k\left(c_{s,k}|_{r_k=1}\right), \qquad k \in n,p, \tag{2.32}$$

Current formulas are given in eqs. (2.33) to (2.35).

$$i_{e,n}\big|_{x=0} = 0, \quad i_{e,p}\big|_{x=L} = 0, \tag{2.33}$$

$$\phi_{e,n}|_{x=L_n} = \phi_{e,s}|_{x=L_n},\ i_{e,n}|_{x=L_n} = i_{e,s}|_{x=L_n} = I \tag{2.34}$$

$$\phi_{e,s}|_{x=L_p} = \phi_{e,p}|_{x=L_p},\ i_{e,s}|_{x=L_p} = i_{e,p}|_{x=L_p} = I \tag{2.35}$$

Concentration in the electrolyte is given in eqs. (2.36) to (2.38).

$$N_{e,n}|_{x=0} = 0, \quad N_{e,p}|_{x=L} = 0, \tag{2.36}$$

$$c_{e,n}|_{x=L_n} = c_{e,s}|_{x=L_n}, \quad N_{e,n}|_{x=L_n} = N_{e,s}|_{x=L_n}, \tag{2.37}$$

$$c_{e,s}|_{x=L-L_p} = c_{e,p}|_{x=L-L_p}, \quad N_{e,s}|_{x=L-L_p} = N_{e,p}|_{x=L-L_p}. \tag{2.38}$$

Concentration in the electrode active material is given in eq. (2.39).

$$N_{s,k}|_{r_k=0} = 0, \quad k \in n,p, \quad N_{s,k}|_{r_k=R_k} = \frac{j_k}{F}, \quad k \in n,p. \tag{2.39}$$

Reference potential is given in eq. (2.40).

$$\phi_{s,cn} = 0, \quad x \in \partial\Omega_{tab,n}. \tag{2.40}$$

Initial conditions are given in eqs. (2.41) and (2.42).

$$c_{s,k}(x,r,0) = c_{s,k,0}, \quad k \in n,p \tag{2.41}$$

$$c_{e,k}(x,0) = c_{e,0}, \quad k \in n,s,p \tag{2.42}$$

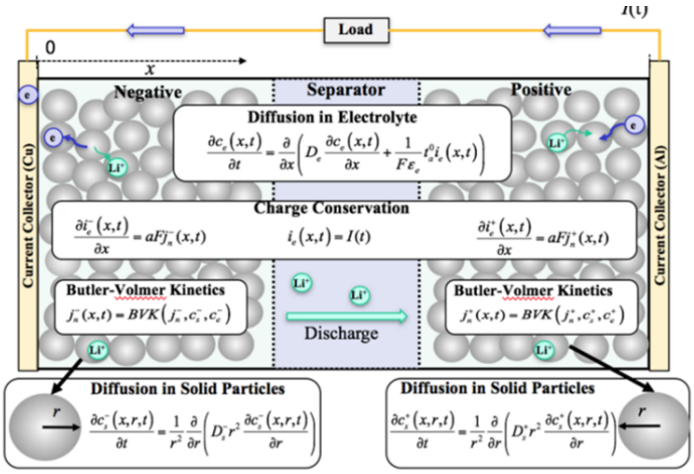

Figure 2.3 : DFN model of Lithium-Ion batteries [2].

2.5 Degradation Modeling

Lithium-ion batteries (LiBs) have undoubtedly reshaped our modern world by initiating a paradigm shift in portable electronics and catalyzing the evolution of electric vehicles (EVs) and stationary energy storage systems. However, as these batteries find applications in increasingly harsh environments, the need for improved performance, longevity and safety becomes paramount. As a result, the scientific community has turned its attention to understanding the complex physics of battery degradation.

During the very long years, numerous reviews have been examined various aspects of LiB degradation, each shedding light on different aspects like diagnosing the degradation, elucidating the effects of cycling conditions, and studying the interplay between various degradation mechanisms. Empirical experiments still achieve to remain important while computational models offer invaluable information, provided they show reliability in predicting degradation events. As the collective behavior often deviates from the sum of its parts, it is very critical that models not only consider individual degradation mechanisms but also account for their complex interactions.

A number of recent computational efforts have attempted to explore the interactions between the degradation mechanisms. Yet, the majority of studies have focused on studying only one pair of mechanisms at a time, neglecting the complexities that result from the simultaneous influence of multiple factors at the same electrode. For instance, there is a lack of direct interactions between more than two mechanisms at a single electrode, although some models rigorously simulate solid-electrolyte interphase (SEI) growth, lithium plating and mechanical stress independently.

In this work, a comprehensive Doyle-Fuller-Newman (DFN) model is investigated using the PyBaMM framework, specifically to incorporate degradation phenomena at the graphite negative electrode. It accounts for the complex mechanisms of crack propagation and particle fracture, as well as the interaction between lithium coating and SEI growth. Collectively, these degradation processes contribute to a range of harmful effects, including loss of lithium inventory, depletion of active material, stoichiometric shifts and impedance changes.

Among the relatively well-understood degradation mechanisms, SEI layer growth, lithium coating and particle breakage are particularly relevant to the graphite negative electrode. Such SEI growth is caused by reactions between the electrolyte and graphite and lithium, leading to lithium compression and increased impedance, thus hindering battery performance.

On the contrary, lithium coating is formed by the accumulation of Li+ ions as Li metal on the graphite surface instead of intercalation, leading to the formation of dead lithium. Though various models have attempted to capture the complex interplay between SEI growth, lithium coating and stripping, none have provided a comprehensive physical explanation.

During cycling, particle breakage as a result of volumetric changes causes mechanical stress and subsequent crack formation, exacerbating degradation by providing additional sites for SEI growth and stimulating active material loss.

The model attempts to integrate these various degradation mechanisms into a unified stress-based framework by considering direct interactions between SEI growth, lithium coating and particle cracking. The integration of these mechanisms into the DFN model provides a better understanding of battery degradation, thus facilitating improved battery design and performance optimization. By supporting advances in LiB technology, this holistic approach promises to enable the realization of safer and

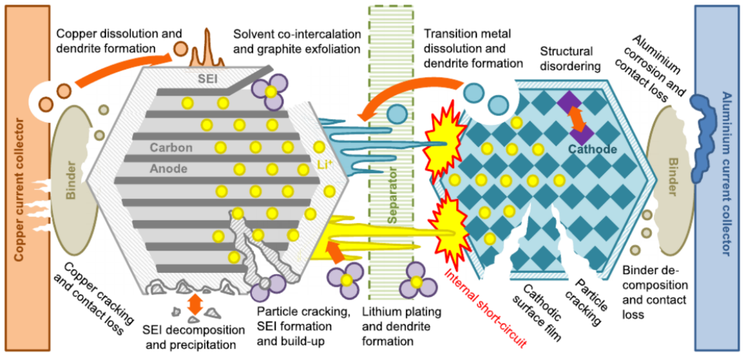

Figure 2.4 : Degradation structure inside Li ion cells [3].

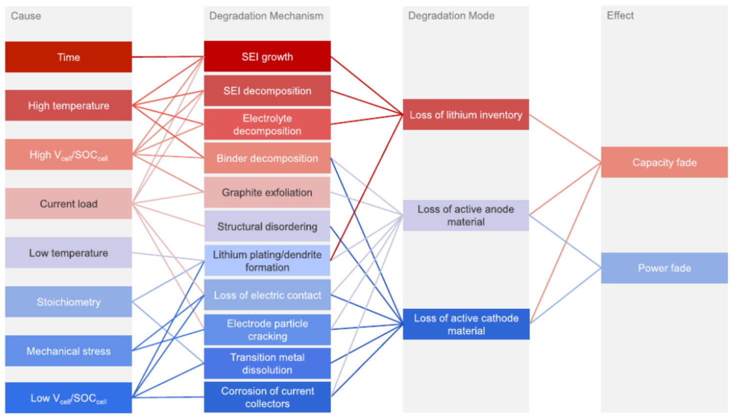

Figure 2.5 : Cause and effect of degradation mechanisms and associated degradation modes [3].

more reliable and long lasting energy storage solutions for a variety of applications [46].

The total lithium loss used in this study is explained as follows. When expressing the total lithium lost, a general approach that can be used with the SPM (Single Particle Model), SPMe (Single Particle Model with Electrolyte), and DFN (Doyle-Fuller-Newman) model is as total lithium lost calculation. When we refer to total lithium loss, it refers to the loss of lithium in the battery and is often related to the detachment of lithium ions from the cathode as well as the anode. Here is how to express this loss as 2.43:

$$TothalLithiumLost = Q_{initial} - Q_{final} \tag{2.43}$$

Here $Q_{initial}$ represents the total amount of lithium at the beginning and Q_{final} represents the amount of lithium remaining after a certain time or cycle. These quantities can be measured in moles. In order to express lithium loss in Ah, we can use Faraday's law. Faraday's law relates the amount of charge carried in an electrochemical reaction to the number of electrons carried and Faraday's constant. Q_{Ah}: Capacity in Ah n: Number of moles of lithium lost F: Faraday constant (96.485 C/mol).For lithium ions, this relationship is as 2.44:

$$Q_{ah} = n \cdot F/3600 \tag{2.44}$$

3. VEHICLE MODELING

The need for co-simulation of batteries and loads during the design phase is crucial to ensure that battery packs can meet performance requirements before significant investments are made. If it uses in the battery packs for EVs, it's more accurate.

The co-simulation not only helps to identify potential design flaws, but also allows engineers to optimise the system in terms of efficiency and performance. By incorporating various components such as the battery management system (BMS), thermal management and charging infrastructure into the simulation, designers can anticipate and mitigate potential problems before they occur. This holistic approach ensures that the final product is robust, reliable and capable of meeting the demands of different driving conditions.

In order to accurately foresee the battery demand, simulations should be performed in various real-world operating scenarios. Simulations for hybrid electric vehicles (HEVs) are highly complex due to the involvement of internal combustion engines, multi speed transmissions and complex hybrid mixing control algorithms which have very complex formulas behind this.

In contrast, simulations for electric-only vehicles (EVs) and plug-in hybrid electric vehicles (PHEVs) are relatively simple. They typically involve internal combustion engines and a single-speed fixed gear system with no power source blending.

The simulation of an electric vehicle requires two main components: an accurate description of the vehicle itself and the function that the vehicle must carry out. The vehicle description covers details about the battery (cell, module, pack), motor, inverter (motor drive power electronics), drivetrain, etc.

The vehicle's function is to follow a desired speed profile versus time, often referred to as a "drive cycle". Examples of drive cycles include the Urban Dynamometer Drive Program (UDDS), the Highway Fuel Efficiency Test (HW-FET), the New York City

Cycle (NYCC), and the US06 drive cycle recorded by the National Renewable Energy Laboratory (NREL) near Golden, CO.

3.1 Approach to Simulating an Electric Vehicle

In the area of vehicle design and simulation, a careful approach is crucial to ensure optimum performance and efficiency. One of the key considerations is the calculation of the desired accelerations in seconds to synchronize with the desired speed of the vehicle. This complicated process covers series of interdependent steps. A vehicle block diagram was followed as shown in figure 3.1.

First of all, the limitations imposed by the engine's acceleration power needs to be considered. These kind of limitations always affect the achievable torque and power values, which are very vital and critical in determining the performance of the vehicle. All these limitations obviously depend on the characteristics of the chosen engine and require careful calibration to match its capabilities.

After determining the achievable torques, the resulting road forces and speed serve it as the cornerstone for their calculation. This calculation is the basis for ensuring that the vehicle's motion is smoothly aligned with the intended speed profile.

Additionally, that engine's power requirements directly affect the battery's performance. Through calculating the battery power according to the engine's demands, the battery's state of charge can be accurately measured, allowing us to accurately measure the battery's SOC and enabling it to monitor and manage energy resources in real time.

By estimating the range of the vehicle based on the rate at which battery energy is depleted, an important aspect of this process is the prediction of the vehicle's range. Such predictive analysis provides valuable information about the vehicle's durability and helps to optimize its operational efficiency.

At its core, a calculation of desired accelerations and related parameters presents the cornerstone of vehicle design and simulation. By refining these calculations, it is by fine tuning performance, maximizing efficiency and driving the future of automotive innovation forward.

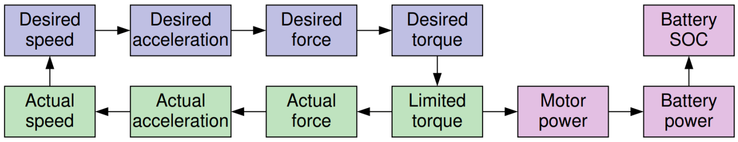

Figure 3.1 : The block diagram of the vehicle model.

3.1.1 Modeling ideal vehicle dynamics

Starting with calculating the desired acceleration force ($D_a[ms^{-2}]$). In order to calculate this desired acceleration force, considering the desired speed is first step($D_s[ms^{-1}]$), which is the main input to the main model. In order to find the desired acceleration speed of the vehicle, subtract the actual speed ($A_s[ms^{-1}]$) from the desired acceleration as in eq. (3.1).

$$D_a = (D_s - A_s)/1[s] \tag{3.1}$$

Then we multiply the desired acceleration by the equivalent mass $E_m[kg]$ to find the net acceleration force. Thus, we get the net desired acceleration force ($D_{af}[N]$) at the road surface as in eq. (3.2).

$$D_{af} = E_m \cdot D_a \tag{3.2}$$

The equivalent mass mentioned in the eq. (3.2) formula above combines maximum vehicle mass ($M_{vm}[kg]$) and equivalent mass of rotating inertias ($M_{ri}[kg]$). Motor inertia ($M_i[kgm^2]$), gearbox inertia ($G_i[kgm^2]$), wheel inertia ($W_i[kgm^2]$), number of wheels (N_w), gearbox ratio ($G_r[N[u/l]]$) and motor RPM and wheel RPM presented as (M_{rpm}), (W_{rpm}) as in eqs. (3.3) and (3.4). Wheel radius ($W_r[m]$) has been assumed to be that of the rolling wheel; i.e., taking into consideration flattening due to load.

$$E_m = M_{vm} + M_{ri} \tag{3.3}$$

$$M_{ri} = ((M_i + G_i) \cdot N^2 + N_w \cdot W_i)/(W_r)^2 \tag{3.4}$$

where gearbox inertia, formula is in eq. (3.5) is measured at motor (not output) side.

$$G_r = M_{rpm}/W_{rpm} \tag{3.5}$$

Four more forces are assumed to act on the vehicle as in eqs. (3.6) to (3.9). Aerodynamic force ($A_f[N]$), air density ($A_d[kgm^{-3}]$), frontal area ($F_a[m^2]$), drag coefficient ($C_d[u/l]$), prior actual speed ($P_{as}[ms^{-1}]$), rolling force ($R_f[N]$), rolling friction coefficient ($C_r[u/l]$) and acceleration of gravity ($A_g[9.81ms^{-2}]$), brake drag force ($B_f[N]$), grade force ($G_f[N]$), constant road force ($C_f[N]$) and grade angle is presented as ($G_a[rad]$). Rolling force is computed to be zero if prior actual speed is zero.

$$A_f = \frac{1}{2}(A_d \cdot F_a \cdot C_d \cdot P_{as}) \tag{3.6}$$

$$R_f = C_r \cdot M_{vm} \cdot A_g \tag{3.7}$$

$$B_f = C_f \tag{3.8}$$

$$G_f = M_{vm} \cdot A_g \cdot \sin(G_a) \tag{3.9}$$

where there is a grade angle or average slope of road (positive is an incline, negative is a decline). In order to compute desired demand torque at motor, demanded motor torque is presented as ($D_{mt}[Nm]$) in eq. (3.10).

$$D_{mt} = W_r \cdot (D_a + A_f + R_f + B_f + G_f)/N[w/l] \tag{3.10}$$

So far it has been analyzed how to calculate desired torque vs. time to match a desired speed vs. time profile. Now, time to place limits on achieved torque based on motor, powertrain limitations. In order to limit the acceleration torque, it is required to define what the available torque is based on the ideal three-phase

AC induction motor model. When positive torque (acceleration) demanded, if prior actual motor speed [$P_{ams}[RPM]$] is lower than rated motor speed ($S_{mr}[RPM]$), then maximum available torque equals rated maximum available torque ($T_{mar}[Nm]$). Or else, maximum available torque [$T_{ma}[Nm]$] computed as in eq. (3.11),

$$T_{ma} = T_{mar} \cdot S_{mr}/P_{ams} \tag{3.11}$$

In order to limit the deceleration torque, when negative torque (deceleration) desired, torque demand split between friction brakes (assume infinitely strong). Energy recovered from motor replaces energy depleted from battery (less inefficiency losses) via regeneration. Maximum (unsigned) motor torque available for regeneration calculated as minimum of maximum available torque for acceleration and a regen fraction times rated maximum available torque. Limited torque at motor is lesser of demanded motor torque and maximum available torque. In order to compute actual acceleration force ($F_{aa}[N]$), the motor torque limits ($T_{lm}[Nm]$) have been established as in eq. (3.12), can compute actual acceleration force that is available, actual acceleration ($A_a[ms^{-2}]$) in eq. (3.13), and actual velocity.

$$F_{aa} = T_{lm} \cdot N[u/1]/W_r - A_f - R_f - G_f - B_f \tag{3.12}$$

$$A_a = F_{aa}/E_m \tag{3.13}$$

The actual acceleration that has just been calculated may cause the motor to rotate at an angular speed higher than its rated value. For this reason, it cannot easily calculate the real velocity. We need to compute a motor speed ($S_m[RPM]$) first, then limit the RPM, and then compute the actual vehicle speed. For this, we need to define the test speed ($S_t[ms^{-1}]$) as in eq. (3.14). Then, limit motor speed ($S_{lm}[RPM]$) by maximum rated motor speed to limit the motor speed as in eq. (3.15).

$$S_t = P_{as} + A_a \cdot 1s \tag{3.14}$$

$$S_m = S_t \cdot N[u/l] \cdot \frac{60[smin^{-1}]}{2\pi[rev^{-1}] \cdot Wr} \tag{3.15}$$

Finally, now that limited motor speed has been calculated, actual vehicle speed is computed as eq. (3.16).

$$A_s = S_{lm} \cdot 2\pi[rev^{-1}] \cdot W_r/60 \cdot N[\frac{u}{l}] \tag{3.16}$$

Equations developed so far show whether vehicle is able to develop accelerations required to follow specific drive profile. In order to understand if the vehicle can advance or follow the required drive profiles, equations are created accordingly. Sufficient battery power is available to supply motor demand is first assumption. In order to decide the range of the vehicle, based on battery capacity, battery needs to be simulated; when a minimum battery SOC or minimum voltage is accomplished, distance that driven to that spesific point is equals to vehicle range. As further, instantaneous power required by the motor ($P_m[kW]$) is calculated by using previous motor speed (S_{mp}) as in eq. (3.17);

$$P_m = (\frac{S_m + S_{mp}}{2}) \cdot 2\pi(rev^{-1}) \cdot T_{lm}/60 \cdot 1000 \tag{3.17}$$

Depending on whether motor power is positive (acceleration) or negative (regeneration/deceleration) battery power ($P_b[kW]$) is calculated as in eq. (3.18) using drive-train efficiency ($E_d[u/l]$) and overhead power ($P_o[kW]$) where overhead power is constant power drain from other vehicle systems, such as air conditioners, infotainment systems etc.

$$(p_b) = \begin{cases} P_o + P_m/Ed, accel. \\ P_o + P_m.Ed, decel. \end{cases} \tag{3.18}$$

Lastly, in order to calculate the battery range ($R_b[km]$) as in eq. (3.20), physics-based modeling is used, where the battery cell current and voltage values are derived from the physics-based model. According to the number of series and parallels in the battery pack, current and voltage are set to pack level, assuming all cells are equal and balanced. After this, using coulomb counting method, battery SOC ($B_{soc}[percent]$) is calculated as in eq. (3.19). Prior battery SOC ($B_{psoc}[percent]$), battery current ($B_cu[A]$), battery capacity ($B_ca[Ah]$), total distance of simulated drive cycle ($D_cs[km]$), maximum rated battery SOC ($B_{maxsoc}[percent]$), minimum rated battery SOC ($B_{minsoc}[percent]$), SOC at beginning ($B_{begsoc}[percent]$) and SOC at end of drive cycle ($B_{endsoc}[percent]$) are used for this calculations.

$$B_{soc} = B_{psoc} - B_{cu} \cdot 1[s]/3600 \cdot B_{ca} \cdot 100[\%] \tag{3.19}$$

$$R_b = D_{cs} \cdot \frac{B_{maxsoc} - B_{minsoc}}{B_{begsoc} - B_{endsoc}} \tag{3.20}$$

4. SIMULATION AND RESULTS

4.1 Comparison of Electrochemical Battery Models

By using the SPM, SPMe and DFN model bases that have been described so far in this thesis, all these models and cell types have been compared for different battery chemistries by using these different modeling techniques with the help of Python Pybamm Library [45] and Matlab platform has been used for the visualizations. Figure 4.1 shows the results of the SPM SPMe and DFN models for a particular chemistry, LFP, using the Pybamm [40]. The model used in this comparison is the default model parameters available in Pybamm and the mesh geometry and cell geometry are chosen by default. These default parameters were obtained from referenced papers [2,39,40,44,45,47,48].

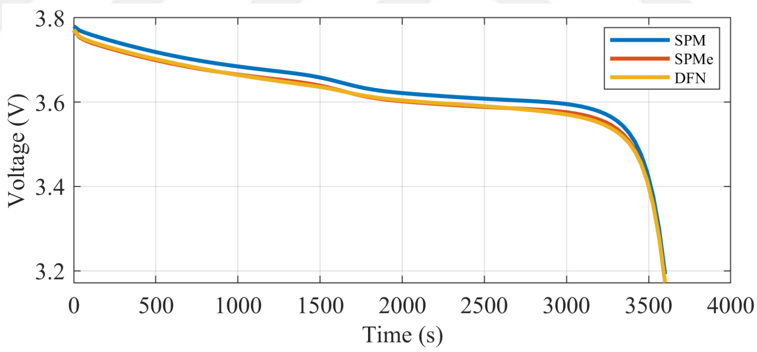

Figure 4.1 : Comparison of 3 different modeling types.

Table 4.1 : Comparison of the computation times of the models.

Model	Computation time (ms)
Doyle Fulle Newman Model	248.25
Single Particle Model with Electrolyte	31.61
Single Particle Model	15.37

In a comparative study on the solution times of the equations for DFN, SPM, and SPMe models, it has been observed that despite using the same solution methodology, the solution time for the DFN model is significantly longer compared to the SPM

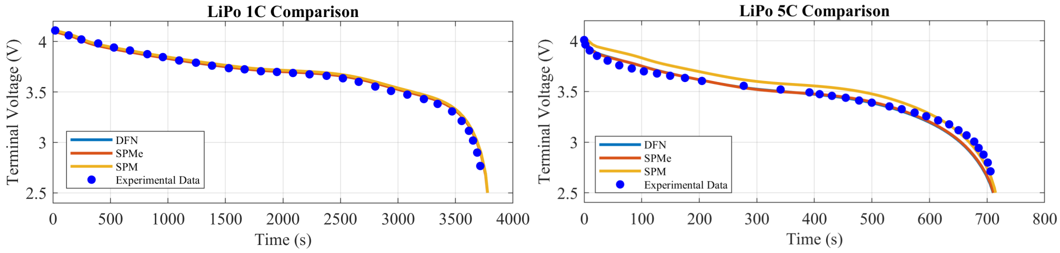

Figure 4.2 : Li-po modeling using DFN, SPMe and SPM model with 1C and 5C C-rates.

and SPMe models. This situation can be explained by the DFN model having a greater complexity in terms of the mathematical representation of the electrochemical processes considered within the model. This complexity directly affects the model's solution time, making it a significant factor in terms of time efficiency in analysis and simulation studies.

First, in Figure 4.2, a comparison of 3 different modeling methods using lithium-ion polymer, Kokam SLPB 75106100, was performed at different C-rates and the total error values were compared. Parameters of the Kokam SLPB 75106100 cell, from the papers [32,33]. The tab placement parameters are taken from measurements in [34]. The thermal material properties are for a power pouch cell by Kokam. The data are extracted from [45]. Lastly, the fits to data for the electrode and electrolyte properties are those provided by Dr. Simon O'Kane in the paper [19]. Also, the experimental data values were obtained from the 1C and 5C discharge values given in the cell datasheet.

Secondly, in Figure 4.3, a comparison of 3 different modeling methods using Lithium cobalt oxide-graphite, Enertech LCOG SPB655060, was performed at different C-rates and the total error values were compared. Parameters for the Enertech cell, from the papers [35,49] and references therein. SEI parameters are example parameters for SEI growth from the papers [49]–[54]. Also, the experimental data values were obtained from the 0.5C and 1C discharge values given in the cell datasheet.

Thirdly, in Figure 4.4, a comparison of 3 different modeling methods using Lithium Iron Phosphate, A123 ANR26650M1B, was performed at different C-rates and the total error values were compared. Parameters of the Kokam SLPB 75106100 cell, from the papers [30]. Subsequently, a re-study was carried out and some of the parameters, in the article [31], were updated to give more accurate results. Nevertheless, it was

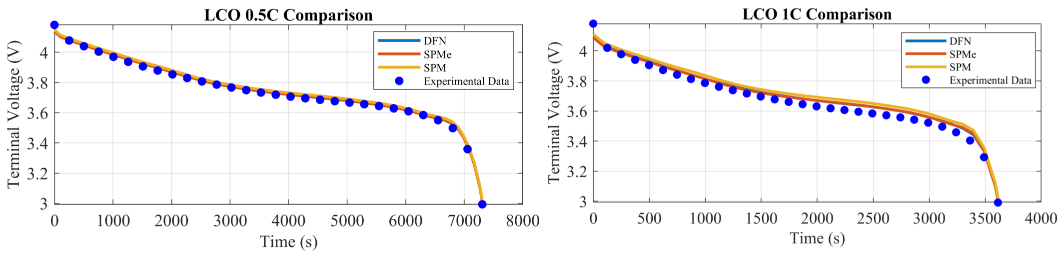

Figure 4.3 : LCO modeling using DFN, SPMe and SPM model with 0.5C and 1C C-rates.

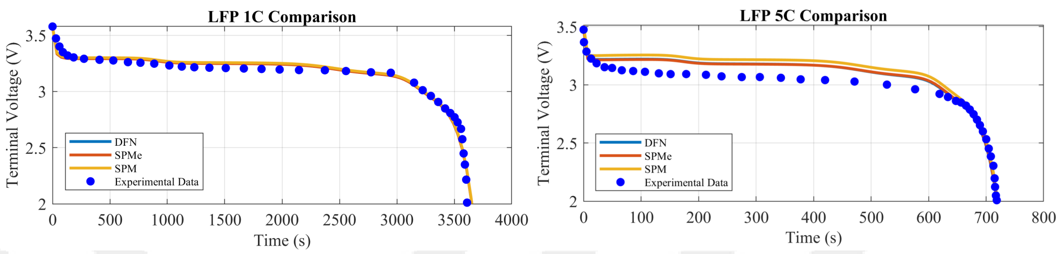

Figure 4.4 : LFP modeling using DFN, SPMe and SPM model with 1C (a) and 5C (b) C-rates.

noticed that even the values in the paper [31] did not exactly match the experimental data, so a parameter optimization technique was attempted. With this parameter optimization technique called curve fitting, curve fitting is the process of generating a curve or mathematical function that best fits a set of data points, possibly subject to restrictions, it was observed that more accurate values were achieved by adjusting the values of Negative electrode thickness and Negative particle radius as in Table 4.2. The rest of the parameters remain the same as in [30].

Fourthly, in Figure 4.5, the modeling of the INR21700 M50 battery cell, which is produced by LG Chem and features NMC 811 chemistry, was conducted. The analysis was carried out at a constant temperature of 25° Celsius, considering two different discharge current rates, 1C and 2C. The Pybamm Chen2020 parameters were utilized as the modeling parameters [55]. Drawing upon the acquired data, it becomes evident

Table 4.2 : Optimized values of LFP model.

	Prada value [30]	Arksand value [31]	Optimized value
Negative electrode thickness [m]	3.6e-5	6.57e-5	3.46e-5
Negative particle radius [m]]	5.86e-6	2.39e-05	7e-7

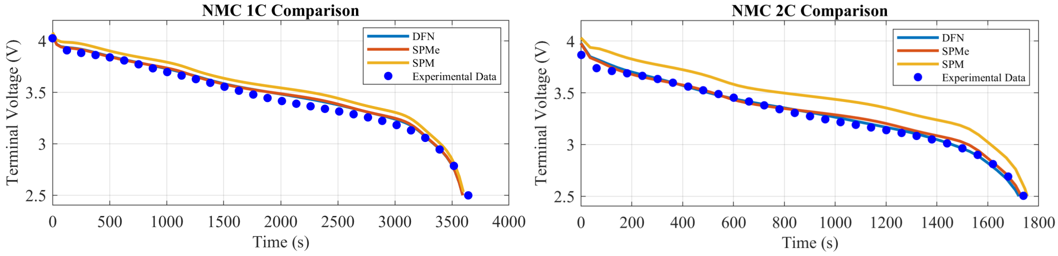

Figure 4.5 : NMC modeling using DFN, SPMe and SPM model with 1C and 2C C-rates.

Table 4.3 : RMS errors (mV) for various battery types and C-rates.

Battery Types	LiPo		LCO		LFP		NMC	
Model / Crates	1C	5C	0.5C	1C	1C	5C	1C	2C
DFN	38.6	66.2	13.3	36.6	65.7	78.2	44.8	34
SPMe	38.8	67	22.8	36.9	66	79	47.5	42.9
SPM	47.6	78.2	25.2	66	66.4	100.9	97	175.3

that the Discrete Fracture Network (DFN) model necessitates extensive mathematical computations and solution time in contrast to the Single Particle Model (SPM) and its extension, SPMe. For LiPo, LCO, LFP, and NMC battery cell types, results obtained using DFN, SMPe, and SPM models at various C-rate values have been compared with experimental data. Root mean square error calculations were performed for each model, and the results are presented in Table 4.3.

As reported in Table 4, the comparison of all these models reveals that DFN has the highest overall score in terms of accuracy. It is followed by SPMe and SPM. Conversely, this order is exactly in the reverse order in terms of complexity and computation time.

4.2 BEV Model and Range Comparison

In this section, a battery electric vehicle model is created using the vehicle modeling method described and explained in chapter 3, and then a detailed simulation study is carried out by combining this vehicle model with the physics-based modeling methods

Table 4.4 : Comparison of each battery model.

Model	DFN	SPMe	SPM
Accuracy	+++	++	+
Complexity	+	++	+++
Computation time	+	++	+++

Table 4.5 : Range Comparison

Drive Cycle	Total Range (with SPM) [km]	Total Range (with SPMe) [km]	Total Range (with DFN) [km]	Test Data [km] [56]
NYCC	52.8	52.2	52.2	51.9
UDDS	62.7	61.9	62.0	62.8
US06	43.7	42.2	42.4	46.7
HW06	63.5	62.9	62.9	63.5

Table 4.6 : Comparison of each battery model.

Drive Cycle	Vehicle model (with SPM) [km]	Vehicle model (with SPMe) [km]	Vehicle model (with DFN) [km]
Simulation Time	7.7826 seconds	20.2555 seconds	35.3894 seconds

described in chapter 2. The modeled vehicle and all its parameters are from the 2011 Chevrolet Volt 1st generation vehicle. In order to test the accuracy of the simulation, the available information and the range data previously performed were compared and results are in Table 4.5. For this comparison, the range information obtained with the data from Argonne Test Laboratory was used together with the information given in the [56] book.

Subsequently, the behavior of each cell in the battery pack when modeled using the battery modeling methods reported in this thesis is examined below. The Pybamm Chen2020 parameters were utilized as the modeling parameters [55] for NMC cell simulation.

First, the SPM cell model was integrated into the vehicle model and simulated to obtain the results shown in Figure 4.6. The results in the graph are divided into 4 sections, each section shows the voltage and current outputs of the cell at a different drive cycle. Also, in the simulation environment created for the SPM model, the total lithium ion loss is shown in Figure 4.7 as the capacity in only one cycle. Total lithium lost refers to the loss of lithium in the battery and is usually related to the separation of lithium ions from the cathode and anode. We can convert this loss into capacity loss as described in Chapter 2 degradation part.

Secondly, the SPMe cell model was integrated into the vehicle model and simulated to obtain the results shown in Figure 4.8. Again, the results in the graph are divided into 4 sections, each section showing the voltage and current outputs of the cell in a

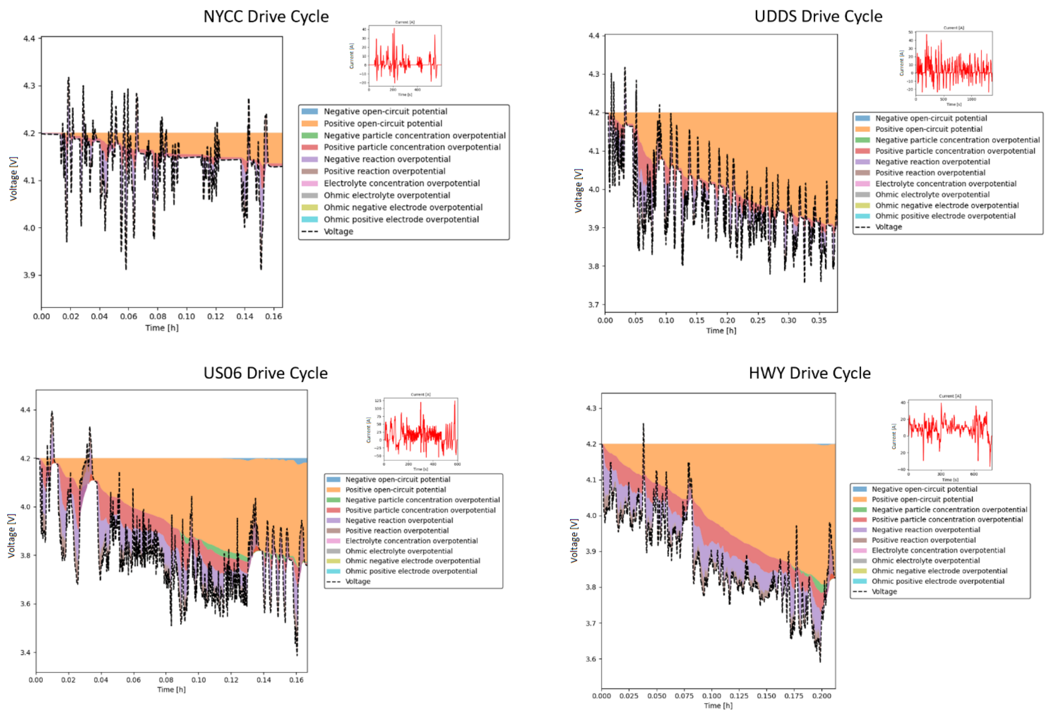

Figure 4.6 : SPM cell model results simulated into the vehicle model.

different drive cycle. Also, in the simulation environment created for the SPM model, the total lithium ion loss is shown in Figure 4.9 as the capacity in only one cycle.

Third and finally, the DFN cell model was integrated into the vehicle model and simulated to obtain the results shown in Figure 4.10. Again, the results in the graph are divided into 4 sections, each section showing the voltage and current outputs of the cell in a different drive cycle. Also, in the simulation environment created for the SPM model, the total lithium ion loss is shown in Figure 4.11 as the capacity in only one cycle.

Finally, a comparison of all these simulations in terms of simulation time duration is shown in Table 4.6.

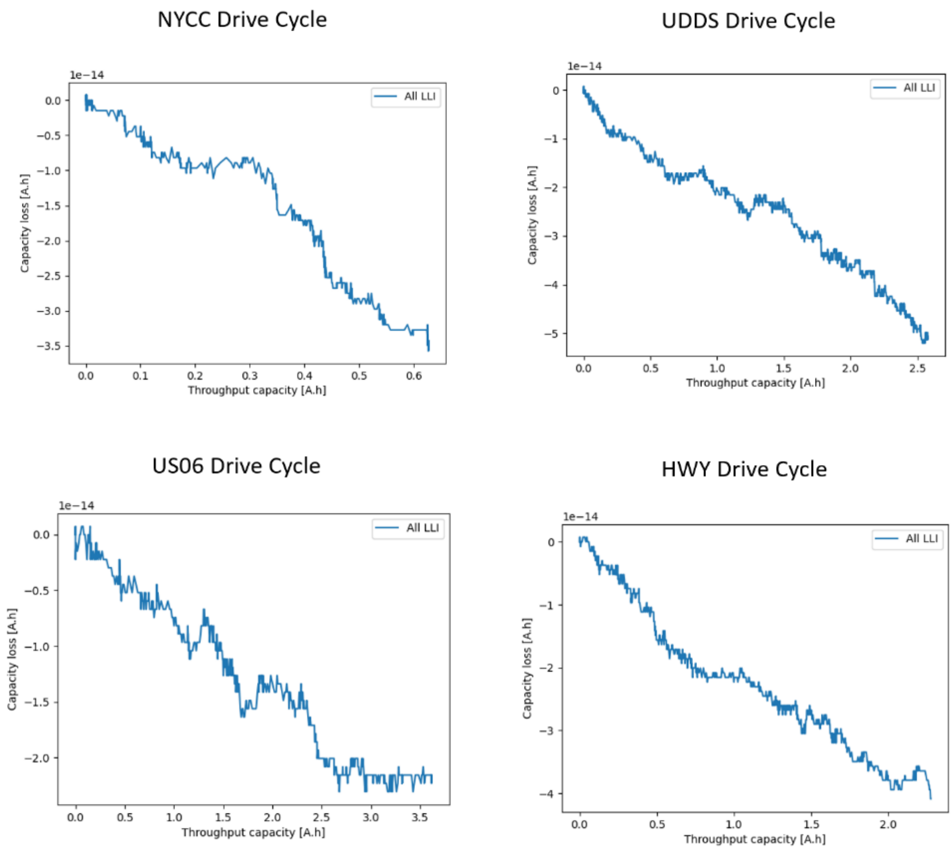

Figure 4.7 : SPM cell model total lithium lost.

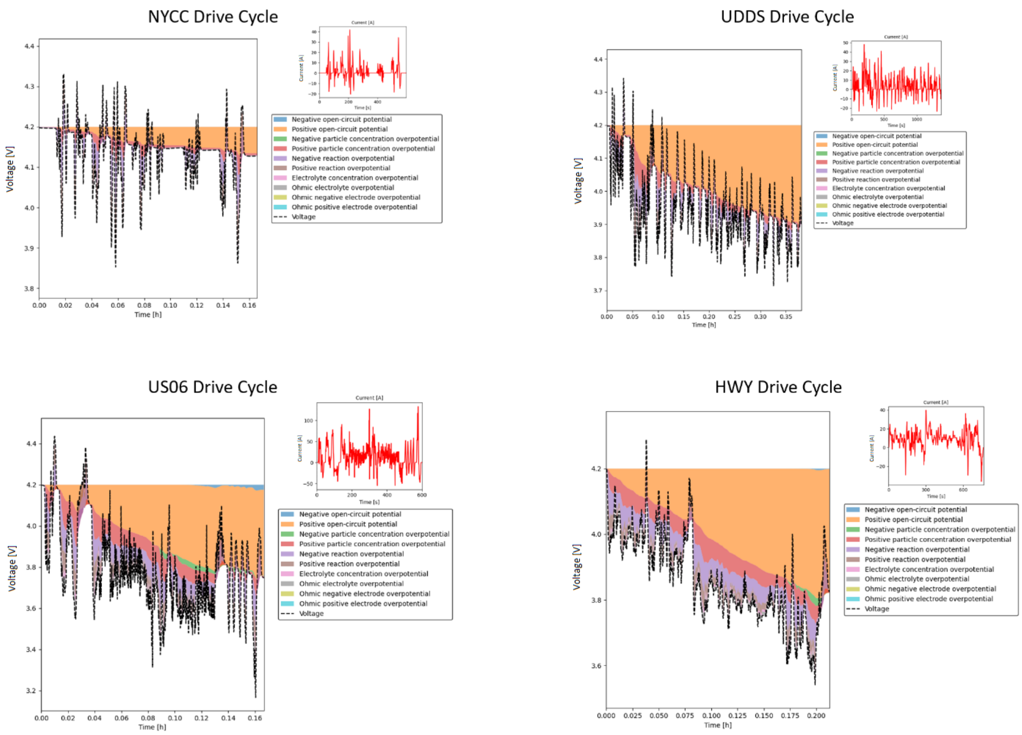

Figure 4.8 : SPMe cell model results simulated into the vehicle model.

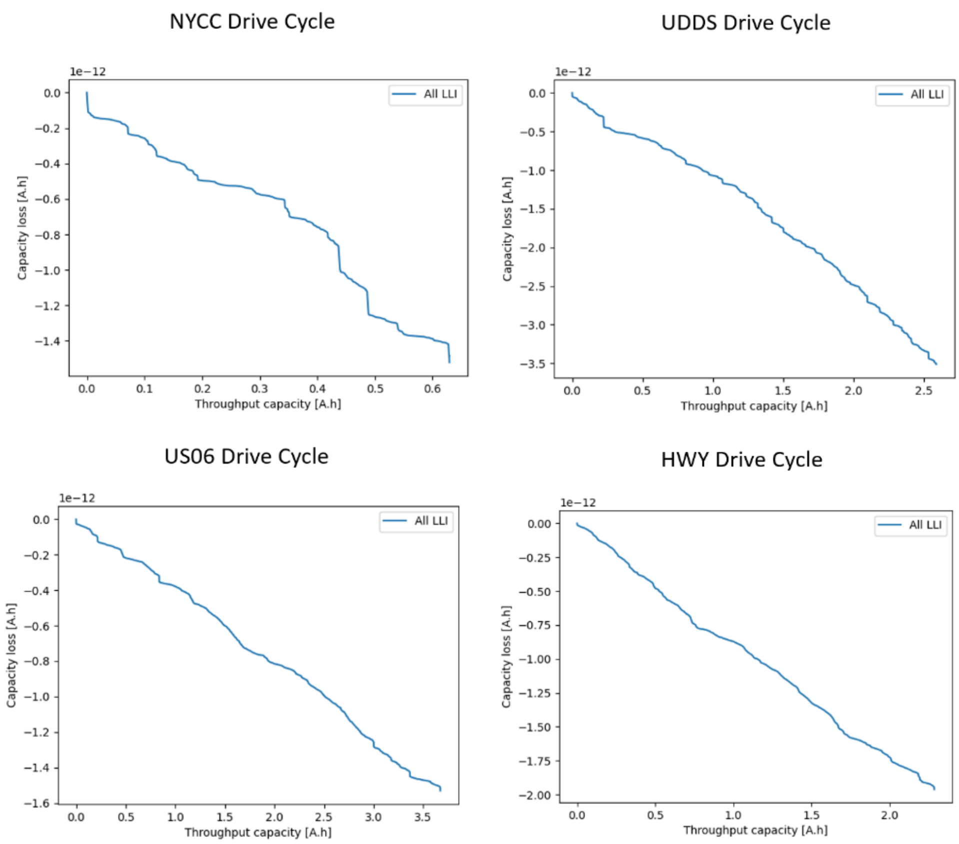

Figure 4.9 : SPMe cell model total lithium lost.

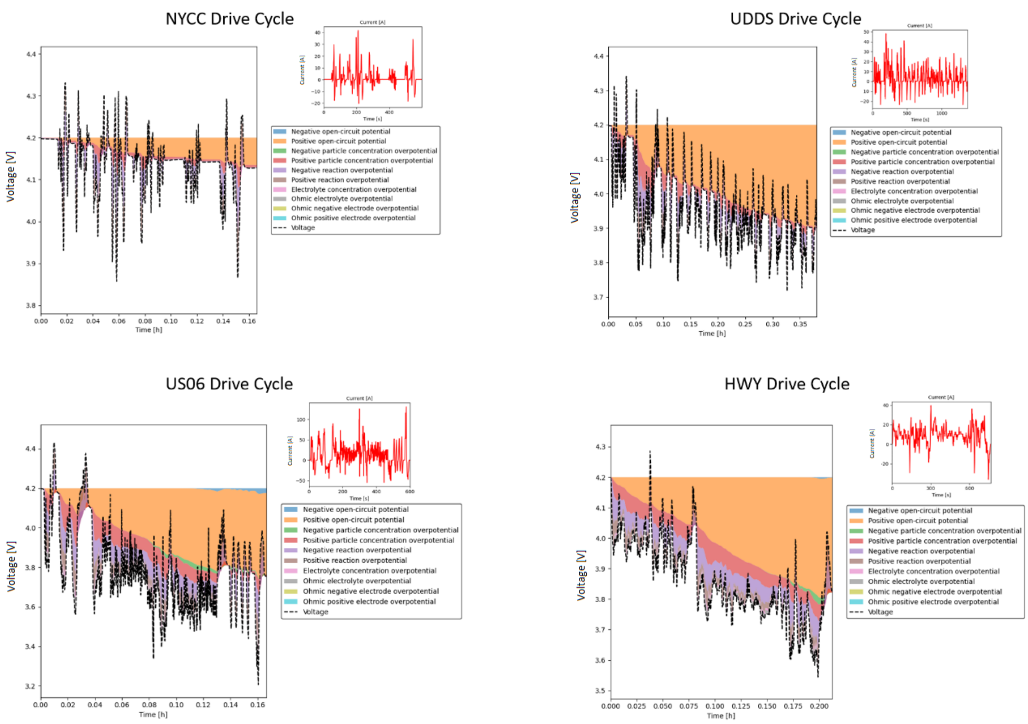

Figure 4.10 : DFN cell model results simulated into the vehicle model.

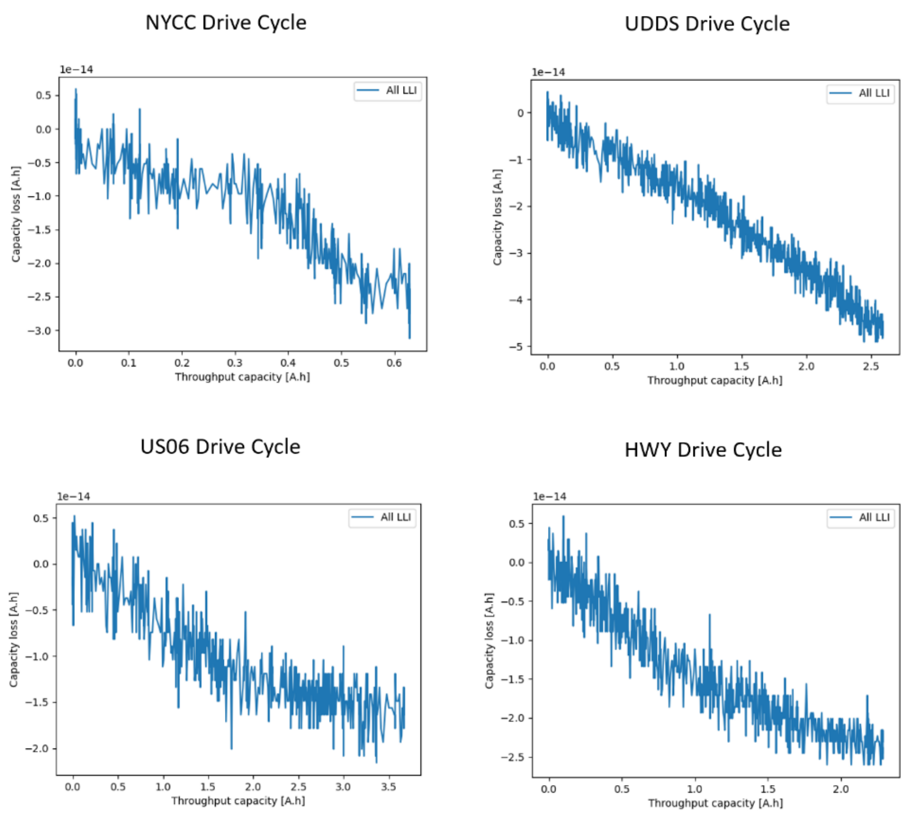

Figure 4.11 : DFN cell model total lithium lost.

5. CONCLUSION

The studies presented and explained in this thesis are hereby concluded with recommendations for future studies.

There are three main concepts that the thesis focuses on:

1. Summarized and compared various modeling methods in existing literature, evaluating their complexity and outcomes, and identified which methods are more suitable for specific chemical systems

2. Updated modeling approaches with optimization methods to enhance accuracy, and investigated the suitability of different chemistries for physics-based modeling.

3. Developed a battery electric vehicle simulation environment using physics-based modeling techniques, calculated range, and analyzed lithium loss to determine capacity degradation.

This study analyzes 3 different electrochemical methods in detail and SPM (Single Particle Model), SPMe (Single Particle Model with Electrolyte) and DFN (Doyle-Fuller-Newman) models offer different levels of accuracy and complexity in simulating lithium-ion batteries. SPM offers simple and fast calculation, but low accuracy by neglecting electrolyte details. SPMe provides higher accuracy by including electrolyte concentration and potential gradients, but the computational complexity is moderate. Although DFN model is very complex and computationally intensive, it offers the highest accuracy. Depends on the application areas and requirements, the model can be chosen accordingly; SPM is more convenient for real-time and fast simulations, SPMe is for applications which requires moderate accuracy and speed, and DFN is for detailed analysis requiring very high accuracy. As expalined in this thesis, different kind of chemistries respond non identical to different electrochemical models. Analyzing which chemistry produces more accurate results in which physics-based model is one of the first inference that can be reached from this study and to decide on the appropriate method by considering the pros and cons. This study gives a short review of the physics-based modeling techniques available in the current literature and compare these modeling techniques in terms of their complexity and predictive capabilities. It also investigates the relationship between these modeling approaches and specific chemical compositions. During the research, various modeling techniques from the literature were refined using optimization methods to improve accuracy. With reviewing the modeling results in detail and after conducting some studies to identify which chemical compositions are more accurately matched to specific modeling methodologies, as well as to identify chemistries more suitable for physics-based modeling. Future research endeavors may prioritize standardizing parameterization procedures and discharge-charge tests within laboratory settings to enhance data precision, while also incorporating machine learning techniques to improve the accuracy of battery parameters. The integration of machine learning and physics-based modeling holds promise for the development of advanced models, facilitating a deeper comprehension of battery dynamics and contributing to the continuous advancement of battery technology. The mathematical calculations required for a vehicle model and the physics-based battery modeling methods that are simulated with this model contribute to real-life sizing studies. In addition, this study examines in detail the loss of lithium, one of the main factors in the aging of a cell, and the associated loss of capacity for each modeling method and simulation. The first conclusion that can be drawn from this is that by using these modeling techniques, it is possible to see in detail how the battery can give results under which loads and to create inputs for all kinds of prediction algorithms. Real-world requirements like climatic conditions, driving profiles and habits and vehicle owners can be investigated to see how cargo load, battery health and the lifespan of electric vehicles can be affected. All this can be combined with real vehicle tests and compared with real data.

REFERENCES

[1] **Brosa Planella, F.**, **Ai, W.**, **Boyce, A.M.**, **Ghosh, A.**, **Korotkin, I.**, **Sahu, S.**, **Sulzer, V.**, **Timms, R.**, **Tranter, T.G.**, **Zyskin, M.** *et al.* (2022). A continuum of physics-based lithium-ion battery models reviewed, *Progress in Energy*, *4*(4), 042003.

[2] **He, W.**, **Pecht, M.**, **Flynn, D. and Dinmohammadi, F.** (2018). A physics-based electrochemical model for lithium-ion battery state-of-charge estimation solved by an optimised projection-based method and moving-window filtering, *Energies*, *11*(8), 2120.

[3] **Birkl, C.R.**, **Roberts, M.R.**, **McTurk, E.**, **Bruce, P.G. and Howey, D.A.** (2017). Degradation diagnostics for lithium ion cells, *Journal of Power Sources*, *341*, 373–386.

[4] **Ding, Y.**, **Cano, Z.P.**, **Yu, A.**, **Lu, J. and Chen, Z.** (2019). Automotive Li-ion batteries: current status and future perspectives, *Electrochemical Energy Reviews*, *2*, 1–28.

[5] **IEA** (2021). Global EV Outlook 2021.

[6] **Sierzchula, W.**, **Bakker, S.**, **Maat, K. and van Wee, B.** (2014). The influence of financial incentives and other socio-economic factors on electric vehicle adoption, *Energy Policy*, *68*, 183–194.

[7] **Barnard, R.**, **Fox, B.**, **Williams, J. and Webber, M.** (2019). Range anxiety, charging infrastructure and vehicle choice: A survey of U.S. electric vehicle consumer experiences, *Applied Energy*, *235*, 1031–1038.

[8] **Bauer, C.**, **Stede, J. and Dallinger, D.** (2017). Consumer requirements for fast charging infrastructure for electric vehicles, *Transportation Research Part A: Policy and Practice*, *103*, 147–163.

[9] **Ellingsen, L.A.W.**, **Majeau-Bettez, G.**, **Singh, B. and Strømman, A.H.** (2014). Life cycle assessment of a lithium-ion battery vehicle pack, *Journal of Industrial Ecology*, *18*(1), 113–124.

[10] **Becker, E.** (2021). A brief history of the electric vehicle, *Tribology & Lubrication Technology*, *77*(10), 74–74.

[11] **Faraz, A.**, **Ambikapathy, A.**, **Thangavel, S.**, **Logavani, K. and Arun Prasad, G.** (2021). Battery electric vehicles (BEVs), *Electric Vehicles: Modern Technologies and Trends*, 137–160.

[12] **Armand, M. and Tarascon, J.M.** (2008). Building better batteries, *Nature*, *451*(7179), 652–657.

[13] **Dunn, B.**, **Kamath, H. and Tarascon, J.M.** (2011). Electrical energy storage for the grid: A battery of choices, *Science*, *334*(6058), 928–935.

[14] **Goodenough, J.B. and Park, K.S.** (2013). The Li-ion rechargeable battery: A perspective, *Journal of the American Chemical Society*, *135*(4), 1167–1176.

[15] **Meng, J.**, **Luo, G.**, **Ricco, M.**, **Swierczynski, M.**, **Stroe, D.I. and Teodorescu, R.** (2018). Overview of lithium-ion battery modeling methods for state-of-charge estimation in electrical vehicles, *Applied sciences*, *8*(5), 659.

[16] **Manwell, J.F. and McGowan, J.G.** (1994). Extension of the kinetic battery model for wind/hybrid power systems, *Proceedings of EWEC*, volume 3, pp.284–289.

[17] **Unnewehr, L.E. and Naser, S.** (1982). Electric vehicle technology.

[18] **Arunachalam, H.**, **Onori, S. and Battiato, I.** (2015). On veracity of macroscopic lithium-ion battery models, *Journal of The Electrochemical Society*, *162*(10), A1940.

[19] **Capasso, C. and Veneri, O.** (2014). Experimental analysis on the performance of lithium based batteries for road full electric and hybrid vehicles, *Applied Energy*, *136*, 921–930.

[20] **Hu, X.**, **Sun, F.**, **Zou, Y. and Peng, H.** (2011). Online estimation of an electric vehicle lithium-ion battery using recursive least squares with forgetting, *Proceedings of the 2011 American Control Conference*, IEEE, pp.935–940.

[21] **Hussein, A.A.H. and Batarseh, I.** (2011). An overview of generic battery models, *2011 IEEE Power and Energy Society General Meeting*, IEEE, pp.1–6.

[22] **Hageman, S.C.** (1993). Using PSpice to simulate the discharge behavior of common batteries, *EDN Mag*, 260–286.

[23] **Karahan, O.**, **Özan, A. and Bağriyanik, M.** The Effects of Mobile Battery Energy Storage Systems on the Distribution Network.

[24] **Alexander, G. and Anton, H.** (2019). Parametrization of a simplified physical battery model, *Proc. 13th Int. Model. Conf., Regensburg, Germany*, volume157, p.2019.

[25] **Li, W.**, **Cao, D.**, **Jöst, D.**, **Ringbeck, F.**, **Kuipers, M.**, **Frie, F. and Sauer, D.U.** (2020). Parameter sensitivity analysis of electrochemical model-based battery management systems for lithium-ion batteries, *Applied Energy*, *269*, 115104.

[26] **Domingos, P.** (2012). A few useful things to know about machine learning, *Communications of the ACM*, *55*(10), 78–87.

[27] **Lucaferri, V.**, **Quercio, M.**, **Laudani, A. and Riganti Fulginei, F.** (2023). A Review on Battery Model-Based and Data-Driven Methods for Battery Management Systems, *Energies*, *16*(23), 7807.

[28] **Watrin, N.**, **Roche, R.**, **Ostermann, H.**, **Blunier, B. and Miraoui, A.** (2012). Multiphysical lithium-based battery model for use in state-of-charge determination, *IEEE Transactions on Vehicular Technology*, *61*(8), 3420–3429.

[29] **Forman, J.C.**, **Bashash, S.**, **Stein, J.L. and Fathy, H.K.** (2010). Reduction of an electrochemistry-based li-ion battery model via quasi-linearization and pade approximation, *Journal of the Electrochemical Society*, *158*(2), A93.

[30] **Prada, E.**, **Di Domenico, D.**, **Creff, Y.**, **Bernard, J.**, **Sauvant-Moynot, V. and Huet, F.** (2013). A simplified electrochemical and thermal aging model of LiFePO4-graphite Li-ion batteries: Power and capacity fade simulations, *Journal of The Electrochemical Society*, *160*(4), A616.

[31] **Arksand, E.** (2021). *Parametrization of a Lithium-ion battery*.

[32] **Ecker, M.**, **Käbitz, S.**, **Laresgoiti, I. and Sauer, D.U.** (2015). Parameterization of a physico-chemical model of a lithium-ion battery: II. Model validation, *Journal of The Electrochemical Society*, *162*(9), A1849.

[33] **Guo, M.**, **Sikha, G. and White, R.E.** (2010). Single-particle model for a lithium-ion cell: Thermal behavior, *Journal of The Electrochemical Society*, *158*(2), A122.

[34] **Hales, A.**, **Diaz, L.B.**, **Marzook, M.W.**, **Zhao, Y.**, **Patel, Y. and Offer, G.** (2019). The cell cooling coefficient: A standard to define heat rejection from lithium-ion batteries, *Journal of The Electrochemical Society*, *166*(12), A2383–A2395.

[35] **Ai, W.**, **Kraft, L.**, **Sturm, J.**, **Jossen, A. and Wu, B.** (2020). Electrochemical thermal-mechanical modelling of stress inhomogeneity in lithium-ion pouch cells, *Journal of The Electrochemical Society*, *167*(1), 013512.

[36] **Ahmadi, M.** (2022). Presentation of the New Method for Simultaneous Estimation of the Parameters and the Charge Situation of Used Batteries in Hybrid Vehicles.

[37] **Raviteja, L. and Gurrala, G.** (2023). A Review of Lithium-ion Battery Physics-based Models, *2023 IEEE Power & Energy Society General Meeting (PESGM)*, IEEE, pp.1–5.

[38] **Zhou, J.**, **Xing, B. and Wang, C.** (2020). A review of lithium ion batteries electrochemical models for electric vehicles, *E3S web of conferences*, volume185, EDP Sciences, p.04001.

[39] **Andersson, J.A., Gillis, J., Horn, G., Rawlings, J.B. and Diehl, M.** (2019). CasADi: a software framework for nonlinear optimization and optimal control, *Mathematical Programming Computation*, *11*, 1–36.

[40] **Marquis, S.G., Sulzer, V., Timms, R., Please, C.P. and Chapman, S.J.** (2019). An asymptotic derivation of a single particle model with electrolyte, *Journal of The Electrochemical Society*, *166*(15), A3693.

[41] **Miguel, E., Plett, G.L., Trimboli, M.S., Oca, L., Iraola, U. and Bekaert, E.** (2021). Review of computational parameter estimation methods for electrochemical models, *Journal of Energy Storage*, *44*, 103388.

[42] **Wang, A., O'Kane, S., Planella, F.B., Le Houx, J., O'Regan, K., Zyskin, M., Edge, J., Monroe, C., Cooper, S., Howey, D.A.** *et al.* (2022). Review of parameterisation and a novel database (LiionDB) for continuum Li-ion battery models, *Progress in Energy*, *4*(3), 032004.

[43] **Jin, N., Danilov, D.L., Van den Hof, P.M. and Donkers, M.** (2018). Parameter estimation of an electrochemistry-based lithium-ion battery model using a two-step procedure and a parameter sensitivity analysis, *International Journal of Energy Research*, *42*(7), 2417–2430.

[44] **Forman, J.C., Moura, S.J., Stein, J.L. and Fathy, H.K.** (2012). Genetic identification and fisher identifiability analysis of the Doyle–Fuller–Newman model from experimental cycling of a LiFePO4 cell, *Journal of Power Sources*, *210*, 263–275.

[45] **Sulzer, V., Marquis, S.G., Timms, R., Robinson, M. and Chapman, S.J.** (2021). Python battery mathematical modelling (PyBaMM), *Journal of Open Research Software*, *9*(1).

[46] **O'Kane, S.E., Ai, W., Madabattula, G., Alonso-Alvarez, D., Timms, R., Sulzer, V., Edge, J.S., Wu, B., Offer, G.J. and Marinescu, M.** (2022). Lithium-ion battery degradation: how to model it, *Physical Chemistry Chemical Physics*, *24*(13), 7909–7922.

[47] **Doyle, M., Fuller, T.F. and Newman, J.** (1993). Modeling of galvanostatic charge and discharge of the lithium/polymer/insertion cell, *Journal of the Electrochemical society*, *140*(6), 1526.

[48] **Deshpande, R., Verbrugge, M., Cheng, Y.T., Wang, J. and Liu, P.** (2012). Battery cycle life prediction with coupled chemical degradation and fatigue mechanics, *Journal of the Electrochemical Society*, *159*(10), A1730.

[49] **Rieger, B., Erhard, S.V., Rumpf, K. and Jossen, A.** (2016). A new method to model the thickness change of a commercial pouch cell during discharge, *Journal of The Electrochemical Society*, *163*(8), A1566.

[50] **Ramadass, P.**, **Haran, B.**, **Gomadam, P.M.**, **White, R. and Popov, B.N.** (2004). Development of first principles capacity fade model for Li-ion cells, *Journal of the Electrochemical Society*, *151*(2), A196.

[51] **Ploehn, H.J.**, **Ramadass, P. and White, R.E.** (2004). Solvent diffusion model for aging of lithium-ion battery cells, *Journal of The Electrochemical Society*, *151*(3), A456.

[52] **Single, F.**, **Latz, A. and Horstmann, B.** (2018). Identifying the mechanism of continued growth of the solid–electrolyte interphase, *ChemSusChem*, *11*(12), 1950–1955.

[53] **Safari, M.**, **Morcrette, M.**, **Teyssot, A. and Delacourt, C.** (2008). Multimodal physics-based aging model for life prediction of Li-ion batteries, *Journal of The Electrochemical Society*, *156*(3), A145.

[54] **Yang, X.G.**, **Leng, Y.**, **Zhang, G.**, **Ge, S. and Wang, C.Y.** (2017). Modeling of lithium plating induced aging of lithium-ion batteries: Transition from linear to nonlinear aging, *Journal of Power Sources*, *360*, 28–40.

[55] **Chen, C.H.**, **Planella, F.B.**, **O'regan, K.**, **Gastol, D.**, **Widanage, W.D. and Kendrick, E.** (2020). Development of experimental techniques for parameterization of multi-scale lithium-ion battery models, *Journal of The Electrochemical Society*, *167*(8), 080534.

[56] **Plett, G.L.** (2015). *Battery management systems, Volume II: Equivalent-circuit methods*, Artech House.

[57] **Yavuz, H.**, **Akyildiz, A. and Gulbahce, M.O.** (2024). A Comprehensive Review of Physics-Based Battery Models and Comparing Different Physics-Based Models for Various Chemistries, *Turkish Journal of Electrical Power and Energy Systems*.

CURRICULUM VITAE

Name SURNAME: HAKKI YAVUZ

EDUCATION:

- **B.Sc.:** 2021, Yildiz Technical University, Faculty of Electrical-Electronics, Electrical Engineering Department

PROFESSIONAL EXPERIENCE AND REWARDS:

- 2021-present, AVL Research and Engineering TR, Battery Development Engineer

PUBLICATIONS, PRESENTATIONS AND PATENTS ON THE THESIS:

- H. Yavuz, A. Akyildiz and M. O. Gulbahce, "A comprehensive review of physics-based battery models and comparing different physicsbased models for various chemistries," Turk J Electr Power Energy Syst., 2024; 4(2), 108-117. [57]